AT8500275

OEFZS BER. No. 4308 RS-245/85 JÄNNER 1985

Österreichisches Forschungszentrum Seibersdorf GesmbH

In-Service Supervision of a Prestressed Concrete Pressure Vessel

Helmut Zemann
Leopold Weißbacher
Norbert Mayer
Claus Amberg

10

ÖFZS Ber.No. 4308 RS-245/84 Jänner 1985

IN-SERVICE SUPERVISION OF A PRESTRESSED CONCRETE PRESSURE VESSEL

Helmut Zemann
Leopold Weißbacher+
Norbert Mayer ++
Claus Amberg

Arbeitsbericht

Österreichisches
Forschungszentrum Seibersdorf
Ges.m.b.H.
INSTITUT FÜR REAKTORSICHERHEIT
Lenaugasse 1o A-1o82 Wien

+ Reaktorbau Forschungs- und Baugesellschaft mbH
++ Bundesanstalt für Materialprüfung Berlin

ÖFZS Ber. No. 4308 RS-245/84 Jänner 1985

IN-SERVICE SUPERVISION OF A PRESTRESSED CONCRETE PRESSURE VESSEL

ABSTRACT

On-line measurements of the physical state of a prestressed concrete pressure vessel and a comparison of the distribution of temperature, strain and stress within the concrete member to the optimized statical predictions and the criterions of layout yield to an efficient and economical method of operating the vessel with a high potential of safety. The requirements of instrumentation and the comparison with static calculations are discussed on the prototype vessel at Seibersdorf Research Center during the phase of construction and prestressing, the phase of the first thermal treatment (stabilization), the pressure tests and under the operating conditions of a high temperature reactor (15o°C/5o bar).

DIE ÜBERWACHUNG UND STATISCHE BEURTEILUNG EINES SPANNBETON-DRUCKBEHÄLTERS WÄHREND DES BETRIEBES

ZUSAMMENFASSUNG

Eine laufende meßtechnische Überwachung des statischen Zustandes eines Spannbeton-Druckbehälters und der Vergleich der realen Temperatur-, Dehnungs- und Spannungsverteilung im Baukörper mit der optimierten prognostizierten Statik und den Auslegungskriterien erlaubt in allen Betriebsphasen eine ökonomische Betriebsführung mit hohem Sicherheitspotential. Am Beispiel des Spannbeton-Prototypbehälters in Seibersdorf werden die instrumentellen Voraussetzungen aufgezeigt und der Vergleich mit der Statik anhand der Bau- und Vorspannphase, der Phase der thermischen Erstbehandlung (Stabilisierung), der Druckprobe und eines Arbeitszyklus unter den Betriebsbedingungen eines Hochtemperaturreaktors (15o°C/5o bar) durchgeführt.

FACHKATEGORIEN: E 13, E 4o, E 41

DESCRIPTOREN: PRESSURE VESSEL/PRESTRESSED CONCRETE/STRAINS/ MEASURING METHODS

CONTENT

1. INTRODUCTION

A Prestressed Concrete Pressure Vessel (PCPV) which is a part of a highly complex system alike a nuclear power plant is expected to meet rigid safety requirements and a high degree of availability. Safety requirements will cover both the structural and design safety of the vessel itself and the operational safety of the plant as far as determinated by the vessel. Operational safety can be gained by adapting the shape of the vessel to the requirements of core design and heat transfer as well as by allowing easy access for the liner and to the internal structures. The intrinsic structural safety of a PCPV - i.e. insensitivity to thermal and pressure overload - will also contribute to the operational safety in an appropriate vessel design. In consequence, the concept of a PCPV with hot liner and adjustable wall temperature [1] will offer major advantages over the cold liner design. Running the liner at the temperature of the reactor coolant avoids insulating problems ("hot spots"). There is no need for dismantling a thermal barrier for liner inspection which results in a remarkable gain not only on safety potential but also in availability.

Estimating the cost of shut down periods on the basis of the deficit of energy production it can be seen, that even a moderate siced HTR-plant of 13oo MWe a 6 to 7 month unproductive period will overcome the total costs of the vessel [1]. From this point of view an extended expense is justified to rise the level of operational safety and availability of the PCPV. This can be done for instance by expanding the temperature control tubing system within the concrete for greater flexibility during transient operating conditions and by an extensive instrumentation and on-line surveillance to monitor the physical state of the vessel. Under close observation advantage can be taken of the facilities of material and design to a greater extent, on the other hand the arise of unexpected or unsafe operating conditions can be detected early enough to take preventive actions against.

To follow this considerations a prototype PCPV with hot liner and adjustable wall temperature was built at Seibersdorf Research Center. The vessel is part of a test facility for high temperature process components which was determinating the shape and the ultimate conditions of continuous operation (1oo bar inner pressure and 3oo°C temperature of process coolant and liner. Behind the liner the temperature level is decreased from 3oo°C to 12o°C within a zone of insulating concrete and is kept between 12o°C and 1oo°C within the prestressed concrete by a temperature control tubing system). The size of the prototype vessel is 12 m high and 3.6 to 4.5 diameter. It is large enough from the modelling point of view for long term temperature tests and load cycles representive for HTR applications.

Four periods of construction and operation have been performed till now

- the period of construction and prestressing
- a one year operation at elevated temperatures up to 12o°C in the structural concrete and the tendons
- pressure tests at 115 bar
- a period of operation under HTR-conditions (5o bar inner pressure and 12o°C liner temperature)

During all periods the prototype PCPV was monitored by an extensive instrumentation. The aim of the measurements was

. to compare the physical state of the vessel with the design calculations

. to run operational tests on steady state and transient HTR conditions

. safety surveillance.

Safety surveillance includes also the supervision of several peripheral equipment (Fig. 1) as there are the external gas supply station, the temperature control system of the vessel and the internal power control. This paper is limited to problems of measurement and the interpretation of data for the supervision of the vessel solely.

2. REQUIREMENTS FOR MEASUREMENT AND INTERPRETATION

For a ciritical examination of the physical state of the vessel from the safety point of view by comparing measurements with statical calculations some basic requirements must be presumed:

- a theoretical description of the physical state must be available on the basis of actual material data, taking into account the load and temperature history of the vessel
- the interpretation of measured data must be founded on an extended knowledge of the properties of the gauges and the influence of instrumental distortion.

Though one may take these statements for granted, both the theoretical description and the interpretation of data are restricted by economic reasons. Without any doubt it is too costly to calculate complete statics for the total live time of the vessel in reasonable small time steps which would be necessary for a complete creep analysis including aging and creep recovery. Moreover, these calculations would be of questionable value, because of the lack of material data. The properties of a certain concrete mix will change with time, temperature and moisture content and the data available for calculations will spread over a wide range depending on the test conditions they are derived from. Since there is no generally accepted creep law available for concrete, these short term data are exptrapolated to a long term fore-cast applying a simplifying mathematical algorithm without physical background. Though this procedure will yield to a reasonable good approximation in the low temperature region - say up to 6o^{o}C when the change of moisture content within the member is neblible all over the life time - it is more dubious or even fails at elevated temperatures when drying occurs. It should be mentioned that even in the low temperature region the use of short term data - especially from dry or drying test specimens - needs some additional optimism to stay on the safe side of static analysis.

Support to the analysis can be gained from long term measurements within concrete members of reasonable large size. Unfortunately there are very few strain, stress and moisture gauges available which are suited for long term measurements at elevated temperatures and they may also introduce some errors by instrumental distortion to an extent which often is underestimated by far. Anyhow, in our opinion, at the present state of knowledge there is no other way to obtain a better understanding of the behaviour of mass concrete members at elevated temperatures than to investigate it by large scale tests in conjunction with parametric studies on concrete properties and gauge behaviour. On the occasion of the construction of the prototype vessel we contemporary performed those tests in a step by step method [1, 2, 3, 4]:

- selective test and improvement of embedded gauges for elevated temperatures
- development of insulating and prestressed concrete investigation of compressive and tensil strength, short term elastic and thermal behaviour
- construction of a large prestressed concrete member representing a 1 m high section of the prototype vessel (test ring) for test purposes
- investigation of long term behaviour of concrete and gauges
- laboratory simulation of a temperature and load cycle performed on the prototype vessel

- recalculation of certain phases of operation of the vessel using concrete properties obtained by long term and simulating laboratory tests
- application of recalculated statics to the safety surveillance of the vessel.

3. TECHNIQUE OF STRAIN MEASUREMENT

For the comparison to the normal layout procedure stress measurements inside the concrete member would be of most importance. Unfortunately, there are very few types of stress gauges available and their application is limited to moderate temperature levels. Besides, they are too bulky to be embedded in a standard cylindrical test specimen of uppermost 3o cm height and 15 cm diameter. So our emphasis was layed on strain measurement though this certainly is introducing an important factor of uncertainty into the evaluation of the stress distribution because of the different strain contributions as there are thermal dilatation, elastic and delayed elastic strains, creep and shrinkage of the material. As a starting point to develop a method for the separation of these contributions we describe the thermally induced variations of the gauge reading by a coefficient $\alpha_G(T)$, which is ideally constant with time. This property may be due to the thermal expansion of the gauge material (housing, vibrating wire, throttle needle etc.) or due to the temperature depending electrical resistance of a resistance strain gauge. This ideal gauge mounted onto a free expanding test specimen with an unknown but time-independent coefficient of thermal expansion $\alpha_C(T)$ will read strains

$$\varepsilon_R = \varepsilon(T) = \Delta T . (\alpha_C(T) - \alpha_G(T))$$

at temperature changes ΔT. If it is possible to determine $\alpha_G(T)$ the thermal expansion of the test specimen can be calculated. Mechanical load applied to the test specimen will add elastic and creep strains $\varepsilon(\sigma, t)$ to the readings $\varepsilon_R = \varepsilon(\sigma, t) + \varepsilon(T)$ which can be evaluated when $\alpha_C(T)$ is known and does not change with load and time. This assumption holds to a very good degree for strain measurements on the liner. $\alpha_C(T)$ is evaluated by mechanical dilatation measurement methods and the gauge calibration is done on test specimen of known thermal and elastic properties. If an individual calibration of the gauge can be applied or a highly uniform manufacturing batch of gauges is available also minor instrumental distortion effects can be taken into account thus allowing a very high degree of accuracy in the interpretation of strain data. (A comprehensive study on instrumental distortion effects is given in /¯5_7). It should be noted, anyhow, that in normal engineering practice strain gauges are adapted to the tested material ($\alpha_G(T)$ equal $\alpha_C(T)$) thus compensating thermal strains and reading only elastic, plastic, restrains etc. in a first approach. At higher temperature loads and in order to investigate the interplay of components of different thermal expansion like concrete and liner thermal dilatations are of interest especially for comparison with design calculations.

Analysis of strains in concrete is more difficult. Changes in the state of moisture either by aging or more pronounced by temperature and drying will introduce shrinkage, creep and a change of the thermal and elastic behaviour. Strictly speaking, "a new kind of concrete grows" - that implies for the analysis of strain data the thermal, load and moisture history should be taken into account, especially when the strains induced by moisture changes are comparable in size to the intrinsic elastic and thermal strains. Parametric studies on concrete properties are limited mostly from the economical point of view, so it seems highly desirable to run test specimen under conditions within as close as possible to the conditions of the concrete of the vessel and to evaluate Young's modulus, shrinkage, creep and $\alpha_C(T)$ for those periods when major changes are expected. The crucial point obviously is to ascertain the comparability of those tests with the state of moisture within the concrete member which implies to control the drying rate of the test specimens. For practical reasons we tried a compromise by

- evaluating the general performance of our concrete mixes in parametric studies
- a detailed creep study of the period of the first thermal treatment
- test specimens within the structural concrete of the PCPV ("dummy gauges").

Information of the gauge properties was gained from those tests by comparing different types and mechanical measuring methods.

The vessel was intended to be equipped with an extensive instrumentation. To follow our general intention in using commercially available components we performed selective tests on different types of embedment gauges at the University of Vienna(TVFA Wien) [2]. Contemporary both embedment strain gauges have been developed and strain gauges for the liner have been tested at "Bundesanstalt für Materialprüfung" (BAM)/Berlin. Several prototype BAM-gauges are in use in addition to the main instrumentation on the PCPV.

3.1 Commercial Embedment Strain Gauges

A variety of commercial embedment strain gauges was investigated for reliability under working conditions to be expected on the PCPV: temperatures up to 3oo°C in a humid and highly alcalic environment. Two types of gauges we finally selected:

	type of gauge	temperature range	concrete structure
A	vibrating wire	15o°C	prestressed concrete
B	resistance	3oo°C	insulating concrete

The performance of these selected types and an additional embedment gauge of mediocre performance (gauge C, vibrating wire type for the use up to 15o°C) are compared in the following.

The first temperature tests have been performed by mounting the gauges in a steel frame (Fig. 2) with a coefficient of thermal expansion very similar to that of the gauges. We suppose this is necessary because without using a mounting unit unpredictable and sudden changes of the readings take place due to bending and internal changes of the prestress of the vibrating wire of the gauge during a temperature cycle. These effects are not typical for operating conditions when the end slabs of the gauge are firmly anchored to the concrete and the tube containing the wire only serves as a housing. Anyhow, the steel mounting unit is less perfect for resistance strain gauges when the housing of the gauges is stretched during a temperature cycle instead of being firmly kept in shape by the surrounding concrete and uniformly strained. This stretching and perhaps some slip of the resistance wire in respect to the housing tube will explain the discrepancy in the observed behaviour of this type of gauges embedded in concrete or mounted in the frame.

5 cycles in steps of 2o°C up to 8o°C and 6 cycles from 8o°C to 12o°C have been performed first. All types of gauges showed an initial hysteresis and a shift of zero reading (Fig. 3) which was neglible for type A and B after the first cycle while type C typically needs 3 to 4 cycles. At the cycles from 8o°C to 12o°C no more shift and hysteresis occured. $\alpha_G(T)$ was evaluated from stable cycles over the entire temperature range (Fig. 4) taking into account the thermal expansion of the steel frame.

Subsequently the stability of reading was examinated over a period of 7oo hours at 12o°C. All types showed some drift of readings. At 3oo°C only type B is still in operation but shows remarcable drift.

The results of the tests are summarized in the following table.

	type A	type B	type C
Thermal coefficient α_G [μm/m°C]	12.2	6.9+ (1o.5)++	11.5
spread of α_G	low	moderate	higher
temperature dependence $\alpha_G = \alpha_G(T)$	very low	low	moderate
drift of reading [μm/m.d] at 12o°C	-o.2±o.1	+o.7±1	o.1±o.3
between 12o°C and 15o°C	2.9±o.5	5.7±3.7	11.2±o.4

\+ not representative for an embedded gauge

++ embedded gauge

The calibration of the gauges is done with the gauges embedded in concrete test specimens (Fig. 5) comparing the readings of the gauge to 4 mechanically measured distance marks on the outer surface of the test specimen. The calibration constants of the gauges are varying widely.

	type A	type B	type C
variation of calibration constant	± 1o%	± 5%, but some specimens -4o to 14o%	± 3o%

Hysteresis under load cycles were observed especially on type B. Long term measurements with the test specimens under load were made over a period of 18o days. We used unsealed test specimens at 2o°C and 45% relative humidity of air in order to come up to a maximum amount of creep and shrinkage. Though there was only a load of 12 N/mm^2 applied on the creep test specimen, first the gauges type C and later type A exceeded their measuring range. While type A returned to normal operation after removing the load, type C completely failed. Type B always was operating properly.

The investigations at elevated temperatures have been made on concrete test specimens stabilized in air for 5oo hours at 2o°C and 45% relative humidity. The tests started with five temperature cycles up to 12o°C with intermediate steps at 6o°C and 8o°C. Next several load cycles have been performed for comparison with thermally untreated specimens. Finally three additional temperature cycles were made to investigate the changes in the thermal behaviour.

The measurements at elevated temperatures include contributions both from the gauge and the concrete. At the very first cycle (Fig. 6) probably some running-in of the gauges occurs in addition to the temperature induced strains of concrete. The latter preponderate when the temperature cycling proceeds and can be interpreted as a change in the coefficient of thermal expansion of concrete and shrinkage.

Shrinkage can be seen in Fig. 6 as an increase of strains during the periods of elevated temperature while a change in the coefficient of thermal expansion of concrete results in a change of the slope (strains per ^{o}C) of temperature steps when they are short enough to neglect shrinkage and gauge drift. This change is neglible during late cycles.

The coefficient of thermal expansion the gauge Type B is compensated for can be evaluated by comparing temperature cycles measured by different types of gauges (Fig. 7). The long term behaviour of the gauges at elevated temperature is overlayed by shrinkage as to be seen in the solid line at 15o^{o}C in Fig. 7. However, the drift of the gauge reading can be estimated with fairly high accuracy by comparison too and is essentially in the same order of magnitude as in the steel frame. The shaded area in Fig. 7 includes the cycles after a 5oo h period at 15o^{o}C. This will give an idea on the short-term repetitional accuracy if one assumes the drying effects on a larger structure to be comparable small like the shrinkage-swelling cycles of a dry test specimen.

In order to test the gauges under more realistic conditions than in dry concrete we built an 1 m high section of the prototype vessel (Fig. 8). Prestress was applied to the member by bottom and top slabs. The temperature level within the concrete is established by a temperature control system similar to the prototype vessel. Different types of gauges including liner strain gauges, mechanical distance marks and BAM-prototype fluidic gauges have been installed in statical equal positions for comparison.

Though, the gauges Type A, B,C performed well under laboratory conditions, they completely failed during the first temperature cycle when the temperature was raised above 80°C because of corrosion and water penetrating into the gauges. The resistance strain gauge (type B) soaked when the soldered connection of the steel sheathing of the cable to the small tubing containing the resistance wire corroded. The vibrating wire gauges (type A) leaked at the clamping of the wire which was sealed by epoxy cement. This situation was found to be typical for most sealants at temperatures near or above 100°C. We had to modify the construction of the gauges and use all-welded closures and connections. In addition we use a vacuum-evaporation system to remove any water from the inner of the gauges. (This also offers less damping of the vibrating wire and in conjunction with a phased-locked-loop exitation system high reliability is gained). The modified gauges work satisfactory since five years.

3.2 Prototype Fluidic Embedment Strain Gauges

The function of fluidic gauges [6] is controlled by the fluid mechanics of the gas flowing through the sensor and the connecting tubes and the corresponding instrumentation. Therefore the main sources of gauge instabilities are geometrical changes of the flow channel boundaries. Material properties are concerned only if they affect geometrical stability. With electrical gauges further properties are important such as the electrical resistivity of permeability. For the construction of fluidic gauges therefore a wider choice of materials is given as for electrical gauges, e.g. the whole sensor can be made out of one corrosion resistant alloy. These fundamental ideas led to the development of fluidic gauges for long term and high temperature applications [5 to 8].

A schematic sectional view of a fluidic embedment gauge for the strain measurement of concrete is shown in Fig. 9. The tube 1 is forced via the flanges 2 to follow the strain ε of the concrete. Hence the guided needle 3 moves within the nozzle 4 controlling the massflow $\dot{m}_M$ forced through this sensing nozzle by the supply pressure p_S. The reference nozzle 5 serves for temperature and pressure compensation. If the thermal expansion of the needle is the same as that of the concrete, than the gauge is temperature compensated. For the instrumentation of the isolation concrete of the PCPV the needles are made from zirconium having a thermal expansion of 5,2 μm/m K (Fig. 11).

A dimensional scheme of the fluidic embedment strain sensor is also shown in Fig. 9. The three fluidic lines coming from the sensor head at the left hand side are made of stainless steel with an inner bore of 1,8 mm. The cap at the right side can be unscrewed to adjust the needle zero-position. It is recommended to fix the sensors and connecting tubes with fine steel wire to the reinforcements or to special wire cages before casting the concrete.

The whole circuit of the fluidic gauge is shown in Fig. lo. It looks like the Wheatstone-bridge well--known from electrical measurement techniques. The left hand half bridge 3 consists of the two sensor nozzles 1 and 2 and the right hand half bridge is formed by the corresponding compensator nozzles 1' and 2'. The compensator needle 4' is automatically positioned by a controller (not shown) within the compensator 5 in such a way that the differential pressure Δp across the bridge becomes zero. Than the position s' of the compensator needle 4' is a linear function of the position s of the sensor needle 4. This relation is mainly unaffected by variations of the supply pressure, the atmospheric pressure, the line resistances R_M, R_S and R_O and the temperatures at all parts of the circuit. This high stability of the fluidic circuit is mainly due to the Wheatstone-bridge concept and the fact, that the sensor nozzles are working under choked conditions, that means the gas flows through the nozzles with sonic velocity. The compensator needle position s' is measured electrically and transformed into an electrical output signal for data processing.

Extensive development had been done especially in the field of long term measurements at high temperatures. With position sensors made from a nickel-base alloy and supplied with argon a thermal zero change of less than $\pm$ o,2% of the measurement range had been measured over a temperature range from 2o to 8oo^{o}C. And at 8oo^{o}C a zero shift smaller than $\pm$ o,2% of the full range per month could be observed. Hence long term stability seems not to be a problem with fluidic strain gauges used for measurements at the PCPV. But to make the best use of this excellent stability it is very important to operate the fluidic circuit under very clean conditions. After some initial trouble with clogged nozzles we now protect each nozzle by an upstream located filter element. Now after many years of measurement experience we can say, that with well designed fluidic circuits there seems to be no problem with pollution.

Fluidic strain gauges embedded within the isolation concrete up to now showed a good performance and very low drift rates. Thus they are qualified for a stable long term PCPV-instrumentation.

3.3 Strain Measurements on the Liner

On the liner strain measurements are performed both on the inner surface and on the concrete side. While the instrumentation at the inner surface is easily accessible and can be changed in case of a failure, the concrete side instrumentation must stand all the lifetime of the vessel. On the other hand the wiring from the inner surface must pass the liner which certainly introduces additional safety problems. We tried both methods using flame spray strain gauges on the inner side for the main instrumentation and selected weldable strain gauges on the concrete side for comparison. All types of gauges are commercially available. In addition to the data given by the manufacturer extensive tests on gauge properties have been performed for the ultimate strain analysis.

3.3.1 Flame Spray Strain Gauges

The choice of flame spray strain gauges for the inner surface was done not only for economical reasons. Preceeding tests proofed their long-term stability and showed neglible hysteresis when applied carefully. Their main disadvantages are the sensitivity to moisture due to hygroscopic backing material and the strong influence of temperature on the strain measurement.

The influence of temperature is twofold - the resistance of the gauge increases and the gauge factor k decreases. Because of the magnitude of those effects it is a must to determine both k and α_G with gauges from the same batch applied on the original liner material. While the decrease of k from 4.57 at 2o°C to 4.15 at 3oo°C is less significant the resistance increases by 7.7 percent over this temperature range which is adequate to a rate of 62 µm/m per °C (Fig. 11). At 3oo°C the temperature dependent readings are five to eight times larger than the restrained thermal dilatation of the liner and up to two orders of magnitude larger than the strains due to the pressure load. To obtain sufficient accuracy of strain data the temperature of the strain gauge should be known better than ± 1°C at 3oo°C. This involves a careful installation of the thermocouples especially at wire connections and at the feed-through out of the vessel because temperature differences along the wiring can cause thermovoltages and severe errors in the temperature correction.

The correction of the temperature influence is linear with temperature in a good approach both for the resistance and the gauge factor. To evaluate the stress distribution from strain data we also use a temperature dependent Young's modulus.

3.3.2 Weldable Strain Gauges

For measurements on the outer liner surface spotwelded fully encapsulated small tube strain gauges /¯9_7 are used in the axial, tangential and diagonal direction. Steel tubes surround the measuring (NiCr or Pt-W) filaments and the integrated electrical leads and protect them against moisture effects and corrosion.

These strain gauges are more expensive than the flame spray type, but their stability not only during the long vessel construction periods but also at high temperatures qualifies them especially for long term measurements in PCPVs. They are easily installed at the liner by spotwelding.

Protective steel covers are used with most of the gauges to prevent direct contact with the concrete and to transmit the forces acting on the liner into the concrete. The reaction to the liner is negligible if the cavity-size is small enough /‾5, lo_7.

The temperature-time behaviour of the gauges generally had been investigated in laboratory tests /‾5, lo and 11_7. Therefore we can eliminate their long term drift and creep errors.

The zero changes α_G due to temperature at free liner expansion had been predetermined by fixing each gauge in a clamping device manufactured from a liner steel probe and than by heating and cooling the device in a furnace (Fig. 11). Thus, α_G of each single gauge is well known too, and the strain gauge readings can be corrected with a small error.

It should be mentioned that some encapsulated NiCr strain gauges had been spotwelded on steel tubes with endplates. These dog-bone shaped concrete strain transducers were radially embedded within the prestressed concrete of the PCPV /‾5_7. Their measuring values are in good agreement with mechanical measurements.

4. INSTRUMENTATION OF THE PROTOTYPE VESSEL

The instrumentation of the vessel which is relevant to structural analysis covers

- temperature measurements within the structural and insulating concrete and on the liner
- strain measurements within the concrete and on the liner
- stress measurements within the prestressed concrete and on the tendons
- measurements of the stability of shape and proportion of the structure
- measurements of the moisture content of concrete

The instrumentation both of stress and strain gauges inside the concrete is done in a very redundant manner. Most of the gauges are located within the "undisturbed region", each type of gauge three times over the circumference in a position which is equivalent from the statical point of view to the position of other types. Strain measurement positions are equipped in three axial or tetrahedral mode. Some gauges are placed also in the bottom and top part of the vessel where stress predictions tend to become complex. These measurements will help to estimate the limits of validity and the necessary amount of calculations.

From different types of embedment strain gauges dummy gauges are made. These gauges are embedded in mechanically insulated concrete specimens within the member. They are sensitive to all temperature and moisture depending strains but not to load dependent strains and can be used to extrapolate for the latter.

Survey of installed instruments and gauges

situation	measured property	type	quantity
Liner	strain	resistance strain gauge	depends on test progr. max. 2oo
Penetrations inside	temperature	thermo-couple	depends on test progr. max. 2oo
Liner on side of concrete	strain	resistance strain gauge	18
	temperature	thermo-couple	7
Insulating concrete	strain	resistance strain gauge	22
		fluidic strain gauge	4
	temperature	thermo-couple	51
		fluidic temperat.gauge	1
Prestressed concrete	strain	integral Bowden strain gauge	
		with LVDT	1
		with potentiometer	4
		vibrating wire strain gauge	13o
		mechanical extensometer	on 12 tendons
		resistance strain gauge	7
	stress	mechanical dynamometer	1o
		hydraulic stress gauge	18
	temperature	thermo-couple	7o
	moisture	neutron probe	21 blind holes
Concrete surface area	deformation	water level	16 positions
		invar scale	16 distances
		optical plummet	2o positions
		hand level	13 points
	strain	mechanical strain meter	21 distances

Tab. 1

The moisture content of the structural concrete was measured by inserting a neutron probe in different depth of blind holes within the member (Fig. 13). Each measuring position should be calibrated separately for absolute humidity measurements because the outer surface or the inner surface of the vessel partially cuts the sensitive area of the probe. Besides, there is a certain amount of non-concrete dead volume due to reinforcement and tendons and the water piping of the temperature control system. For sake of simplicity we use relative humidity data related to the local moisture distribution at the beginning of concrete work to compare with test specimen data.

Fig. 12 shows a survey of the mainpositions of the instrumentation. In Tab. 1 the different measuring systems are listed. Fig. 14 schematically gives an impression of the size of stress and strain gauges in comparison of the "fine structure" of the concrete member as there are tendons, reinforcement and the temperature control tubing. This relation of size should be kept in mind when discussing the results of measurements.

5. IN-SERVICE SUPERVISION OF THE PCPV

5.1 Prestressing the PCPV

During the phase of prestressing we had the opportunity to compare predicted data to the real structure the first time using the arise of prestress as a functional test of the gauges over the entire measuring range. Fig. 15 shows a set of stress data measured directly by stress gauges and computed from strain measurements in comparison with the predicted stress distribution over a cross section with completely applied prestress. There seems to be some scattering in the results but in a more detailed study it appears that this is due to the "fine structure" of the member (Fig. 14). The simplified computing algorithm we used could not predict local zones of higher stress near the tendons but both strain and stress measurements in equivalent positions did detect it. This seems of some interest for zones on top and bottom of the vessel and near the penetrations where a recalculation for every phase of operation will become very expensive. Besides, it will give an idea on the bandspread of stress inside the member. During the subsequent phase the PCPV was on low temperature level. Moderate loss of prestress could be observed until the begin of the first high temperature cycle where an increased loss of prestress occured (Fig. 16). Unfortunately the stress gauges failed at about 8o^{o}C, so our further investigations are based on mechanical and electrical strain measurements and stress measurements on the tendons only.

5.2 The Phase of Stabilization

Running the structural concrete at elevated temperatures loss of prestress is expected both from relaxation of the tendons and from creep. As we know from our laboratory investigations, the main changes in material properties and most of the creep takes place during the first temperature cycles when the concrete is allowed to dry. In order to anticipate the major losses of prestress during the first temperature cycle, we planned to force the free surface evaporation of surplus water by vacuum evaporation via a system of drying holes inside the member.

Fig. 17 shows this first temperature cycle comparing temperature, loss of prestress, loss of moisture and strains on the outer surface of the vessel. The temperature was raised in steps up to 12o^{O}C and kept on this level for three months. Loss of moisture was greatest between 8o^{O}C and 1oo^{O}C so most of the evaporable water was already removed at the beginning of the 12o^{O} period. Loss of prestress is in close correlation to the loss of moisture. (There is also a loss of prestress due to the thermal expansion of the tendons which is gained again at decreasing temperature. This loss had been substracted in this figure for sake of transparency). The effect of drying on mechanically measured strains is overlayed by thermal expansion at increasing temperature level but can be seen at constant temperature for instance at 12o^{O}C. An electrical measurement (Fig. 18) of strains inside the structural concrete will give a better impression on drying effects because the gauge partially compensates the thermal expansion of concrete. The observed strains therefore contain creep, shrinkage, thermal expansion and imperfect α-matching.

Fig. 18 compares a triaxial strain measurement to a dummy gauge. All gauges behave similar except different concrete creep contributions. The dummy only reacts on temperature and shows strains due to shrinkage and the difference between the coefficient of thermal expansion of gauge and concrete. It can be used to separate the latter from other gauge readings. In order to separate the different contributions we performed creep tests using sealed and unsealed specimens we had cast with the original concrete. The testing parameters are set as close as possible to the physical state of the prototype vessel. The same temperature history is performed with one exception: at significant steps - before the temperature on the PCPV is raised - the temperature of the test specimen is reduced for a short time to ambient temperature. As an example Fig. 19 compares strains during the temperature cycle measured both by an electrical and a mechanical gauge. At elevated temperatures, pronounced creep and a change of the coefficient of thermal expansion takes place, resulting as well in a negative drifting top of the cycle as in a drifting 2o^{o}C base line. The difference of the base line of mechanical and electrical gauge is due to gauge drift and a gauge factor different to the specification of the manufacturer. To separate the effect of a change of the coefficient of thermal expansion, one may plot strains in relation to temperature similar to Fig. 6 (Fig. 2o). The slope of the cycle of these electrically measured data represents the difference between gauge and concrete in the coefficient of thermal expansion. At the 2o°C level residual creep strains appear when the cycling proceeds. When the specimen is unsealed this cycling finally enters into a loop between shrinkage and swelling.

Fig. 21 shows the observed variations of moisture within the member averaged from measurements in equivalent positions from the beginning of concrete work to the end of the phase of stabilization. Minor long term changes take place at ambient temperature. The main loss of moisture starts at about 8o°C and nearly is finished at the beginning of the 12o°C period.

The most interesting part of this curves is the 12o° period, when the concrete properties tend to stable conditions. In order to estimate the necessary length of stabilization time one may use a semilogarithm time-plot of the columetric moisture concent (Fig. 22). The correlation of the concrete properties to moisture gained from test specimen will help to set a practical limit of drying time. We have even 14 weeks at 12o°C while the water content decreased from 8.8 to 6.6 percent of volume. Another 14 weeks at 12o°C will give about o.8% loss with tolerable changes of concrete properties.

5.3 Pressure Tests

After the phase of stabilization we represtressed the prototype vessel and performed several cold pressure tests up to 115 bar at 5o°C liner temperature. The stress distribution (Fig. 23) computed from triaxial strain measurements inside the concrete during this load cycles again is in good agreement with the predicted values.

5.4 HTR-Temperature and Pressure Cycle

Finally we started an operational temperature and pressure cycle (Fig. 24 a) to test the prototype vessel as a HTR-PCPV. This cycle is started with a pressure test for tightness. Then the temperature of the PCPV was raised. The liner was heated up to 12o ^{o}C while the structural concrete was kept on 8o ^{o}C. At this temperature level a first load cycle with 5o bar inner pressure was performed. After this, the inner pressure was reduced to 1.5 bar. The liner temperature was raised to 15o ^{o}C and temperature of the structural concrete to loo ^{o}C. As an example Fig.24 b shows triaxial strains measured by electrical gauges and a dummy gauge. The gauges behave similar to the phase of stabilization and mainly show thermal strains. The elastic strain peaks both from the 35 and 5o bar pressure load test are small compared to the thermal expansion readings. If we assume the dummy gauge is as much imperfect adapted to the surrounding concrete in respect to the coefficient of thermal expansion as the active gauges are, information on the actual coefficient of thermal expansion can be gained from a thermal cycle short enough to expect no additional residual strains. On the other hand substraction of the dummy reading from the other readings will yield to temperature compensated strains, (Fig. 24 c). In this plot the strain peaks due to the pressure load can be seen more clearly. The predicted strains for the 5o bar pressure cycle are in good agreement with our measurements. When the temperature of the vessel was raised to loo^{o}C additional strains with decreasing rate occured. This is due to the drying of the insulation concrete because drying induced strains in this zone yield to a static reaction of the prestressed concrete.

The zone of insulation concrete is fairly small compared to the prestressed member, so the resulting strains within the structural concrete are small too and tend to stable conditions when the drying of the insulation concrete proceeds.

In conclusion, the prototype vessel can be monitored in all periods of operation by the embedded instrumentation. The measurements are interpretable to a high extent.

They can be used both for safety surveillance - to detect unsafe or unexpected operating conditions - and to estimate the limit of validity and the necessary amount of design calculations.

LITERATURE

/¯1_7 Német, J., Fritz, K.:
Concept, Construction, Testing and Operational Safety of a PCPV with Elastic Hot Liner and Adjustable Wall Temperature
SMIRT 5th, Paper H 6/1, Berlin, Aug. 1979

/¯2_7 Német, J., Zemann, H.:
Untersuchungen über elektrische Dehnungsaufnehmer für das Innere von Beton bis 12o °C bzw. 3oo °C
SMIRT 2nd, Paper H 4/9, Berlin 1973

/¯3_7 Weißbacher, L., Német, J., Zemann, H.:
Properties of Concrete at Elevated Temperatures
SMIRT 5th, Paper H 1/1, Berlin, Aug. 1979

/¯4_7 Zemann, H., Weißbacher, L.:
PCPV Instrumentations and Measurement Techniques at Elevated Temperatures
IAEA-Techn.Com. Meeting on Vessel Concepts for Gas-Cooled Reactors
Lausanne, October 1978

/¯5_7 Czaika, N., Mayer, N., Amberg, C., Magiera, G., Andreae, G., Markowski, W.:
Zur Meßtechnik für die Sicherheitsbeurteilung und -überwachung von Spannbeton-Reaktordruckbehältern.
Dt. Ausschuß für Stahlbeton, Schriftenreihe, Heft Nr. 293, Berlin 1978
Also published as research report No. 5o by Bundesanstalt für Materialprüfung, Berlin 1978

/¯6_7 Mayer, N., Rohrbach, Chr.: Handbuch für fluidische Meßtechnik.
VDI-Verlag, Düsseldorf 1977

/¯7_7 Mayer, N., Flesch, U.:
A Fluidic Strain Measuring System for Prestressed Concrete Reactor Pressure Vessels
5th Cranfield Fluidics Conference, Uppsala 1972, Paper A 1

/¯8_7 Mayer, N.:
A Fluidic System for Longterm Measurements of Several Variables in High-Temperature Nuclear Applications
2nd Intern.Conf.onf "Struct.Mech.in Reactor Techn.", Berlin 1973, Paper H 4/11

/¯9_7 Gibbs, J.:
Two Types of High-Temperature Weldable Strain Gauges: NiCr Half-Bridge Filaments and Pt-W Half-Bridge Filaments.
Exp.Mech. 7(8) pp 19A - 26A (1967)

/¯1o_7 Czaika, N., Mayer, N., Amberg, C., Magiera, G.:
Instrumentation for Use in Prestressed-Concrete Reactor Pressure Vessels.
Exp.Mech.Febr. 1974,pp. 82-88

/¯11_7 Amberg, C., Czaika, N.:
Über das langzeitige Drift- und Kriechverhalten gekapselter, aufschweißbarer Dehnungsmeßstreifen mit NiCr-Meßdraht bei Temperaturen bis 32o °C.
VDI-Bericht Nr. 399, 1981, pp. 1o5-111

FIGURES

Fig. 14: Gauges inside the structural concrete

A liner
B insulating concrete
C prestressed concrete
D tendons
E reinforcement
F temp. control tubing
G stress gauge
H vibrating wire gauges
H' vibrating wire dummy gauge
J resistance strain gauges
K thermocouples
L Moisture measuring position, arrow indicates sensitive volum

Fig. 15: Comparison of predicted stress distribution to stress measurements and the stress distribution calculated from strain measurements

Fig. 16: Stress history from prestressing to the phase of thermal stabilization

Fig. 17: The phase of stabilization

Fig. 18: Phase of stabilization: strain readings from a set of triaxial and dummy vibrating wire gauges inside the prestressed concrete

Fig. 19: Laboratory simulation of the phase of stabilization to evaluate the changes of concrete properties

Fig. 2o: Creep and change of thermal expansion - laboratory simulation of the phase of thermal expansion

Fig. 21: History of moisture distribution inside the prestressed concrete

Fig. 22: Drying of the prestressed concrete at 12o ^{o}C (phase of stabilization)

Fig. 23: Pressure tests - comparison of predicted and measured stress distribution

Fig. 24: HTR-cycle a) history of temperature and inner pressure load

b) strains measured by vibrating wire strain gauges

c) temperature compensated strains (comparison of measurement and calculation for the inner pressure load)

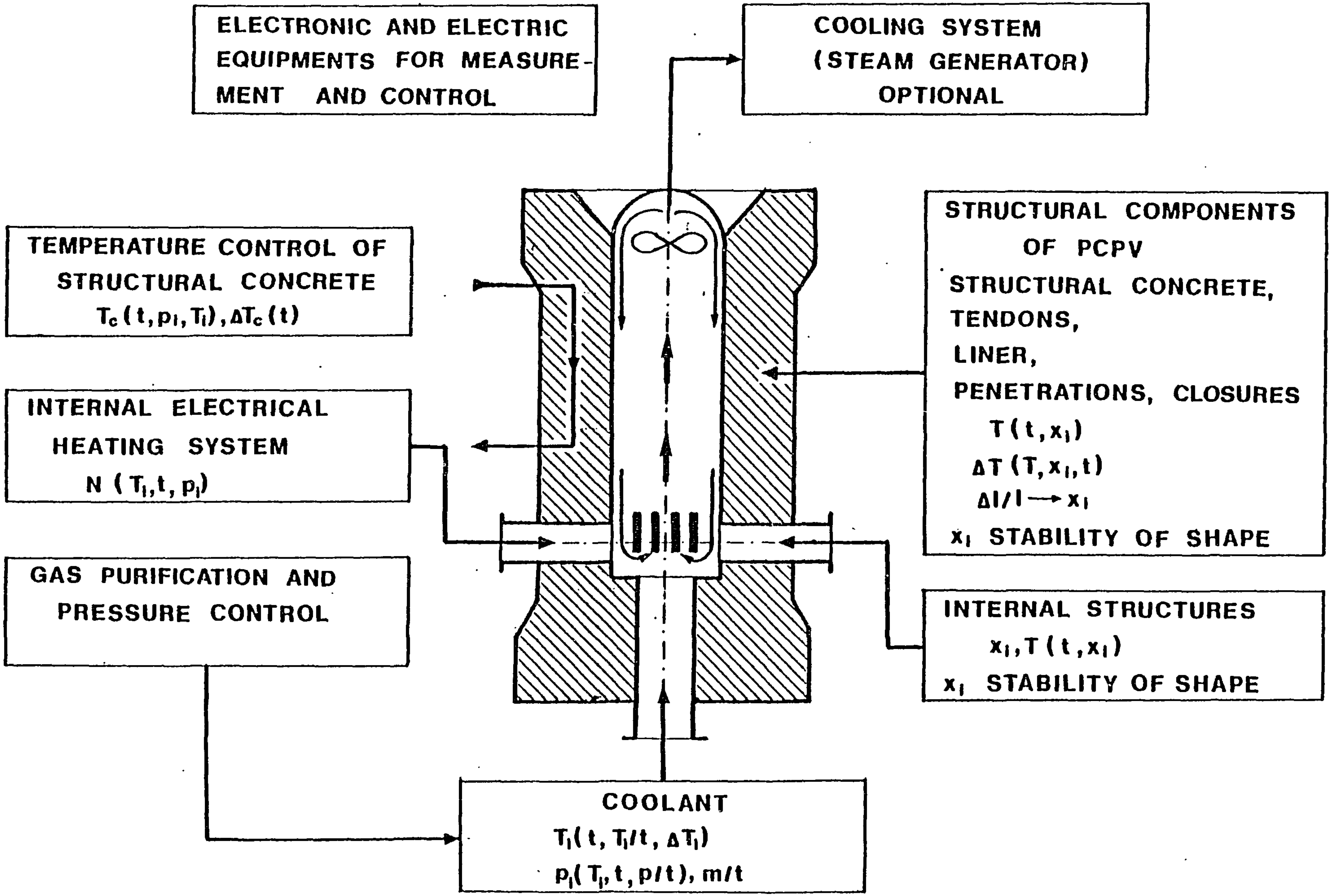
ELECTRONIC AND ELECTRIC EQUIPMENTS FOR MEASUREMENT AND CONTROL
COOLING SYSTEM (STEAM GENERATOR) OPTIONAL
TEMPERATURE CONTROL OF STRUCTURAL CONCRETE
$T_c(t, p_l, T_l), \Delta T_c(t)$
STRUCTURAL COMPONENTS OF PCPV
STRUCTURAL CONCRETE, TENDONS, LINER, PENETRATIONS, CLOSURES
$T(t, x_l)$
$\Delta T(T, x_l, t)$
$\Delta l/l \rightarrow x_l$
x_l STABILITY OF SHAPE
INTERNAL ELECTRICAL HEATING SYSTEM
$N(T_l, t, p_l)$
GAS PURIFICATION AND PRESSURE CONTROL
INTERNAL STRUCTURES
$x_l, T(t, x_l)$
x_l STABILITY OF SHAPE
COOLANT
$T_l(t, T_l/t, \Delta T_l)$
$p_l(T_l, t, p/t), m/t$

Fig. 1

Fig. 2

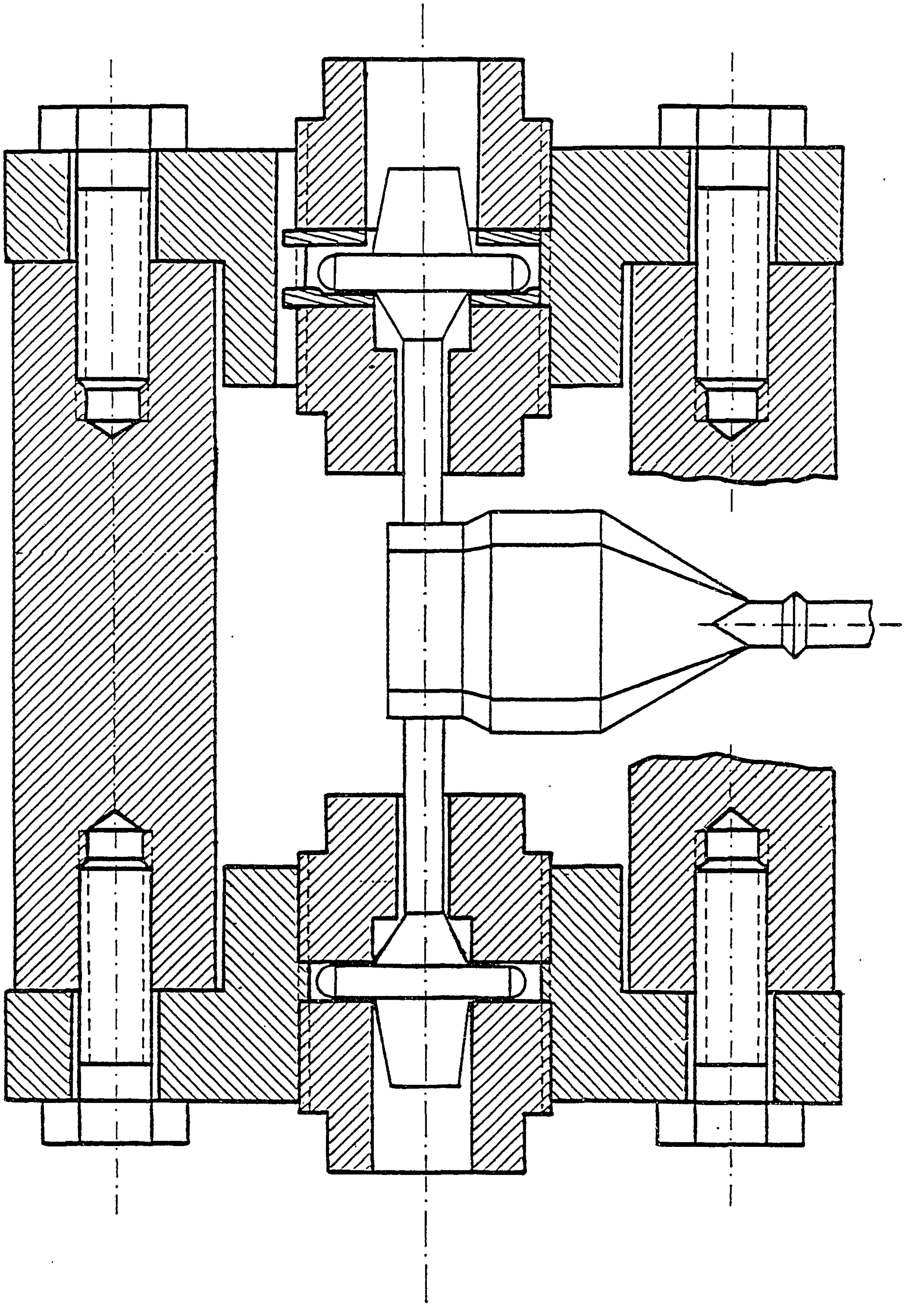

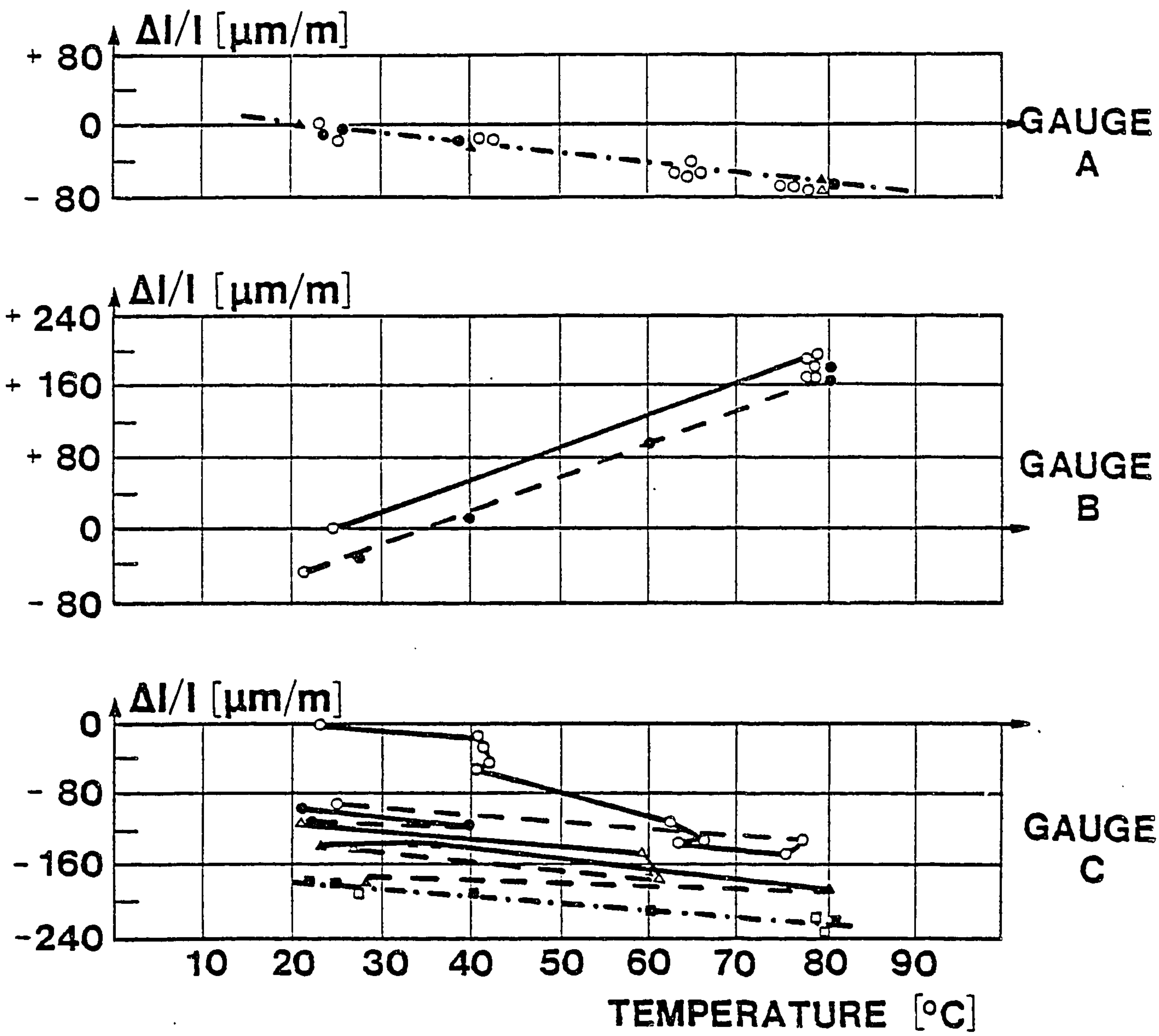

TEMPERATURE CYCLES	SYMBOLS
1.	○
2.	●
3.	△
4.	▲
5.	□
6.	■

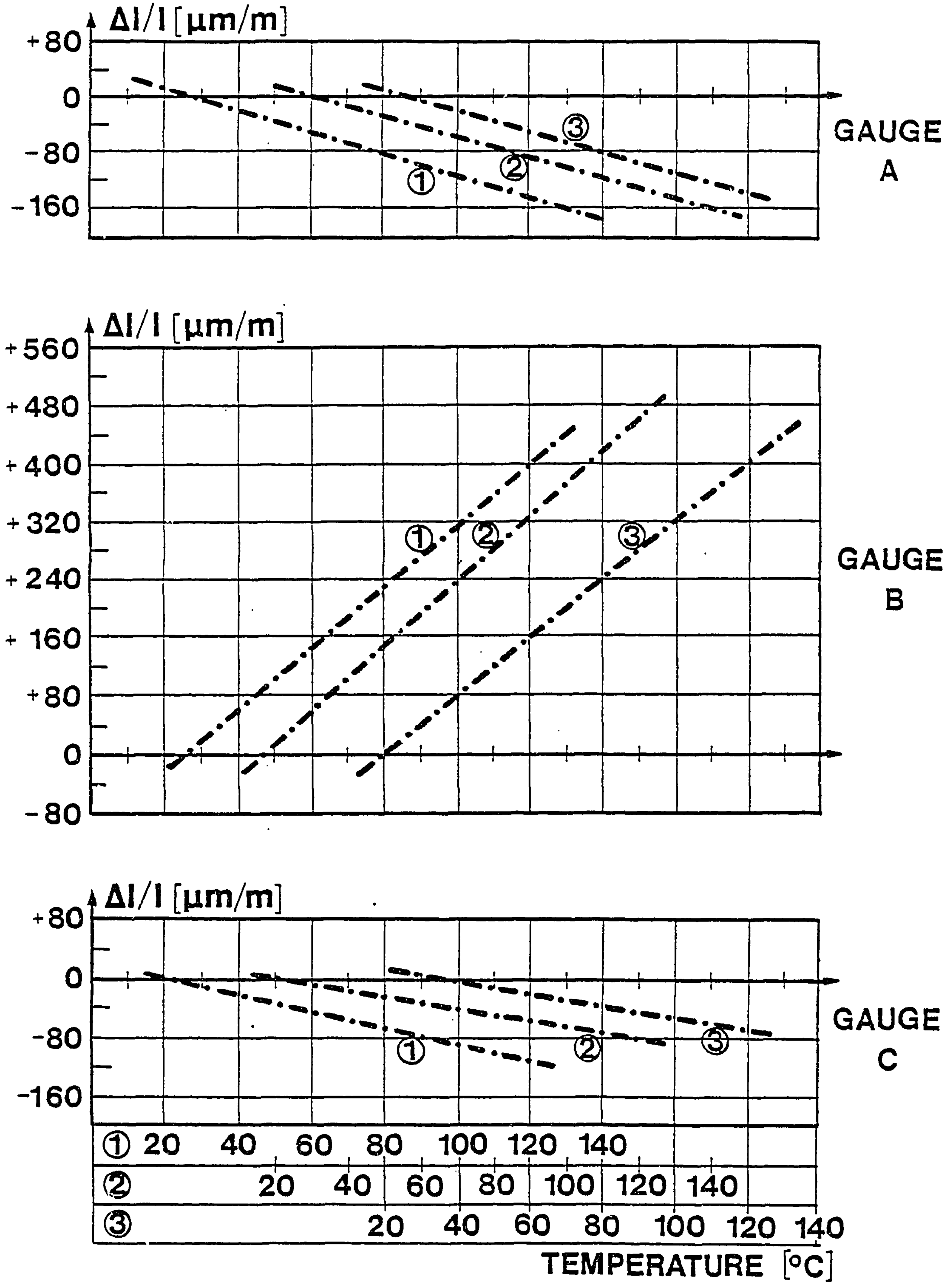
Δl/l [μm/m]
+80
0
-80
-160
GAUGE A
Δl/l [μm/m]
+560
+480
+400
+320
+240
+160
+80
0
-80
GAUGE B
Δl/l [μm/m]
+80
0
-80
-160
GAUGE C
① 20 40 60 80 100 120 140
② 20 40 60 80 100 120 140
③ 20 40 60 80 100 120 140
TEMPERATURE [°C]

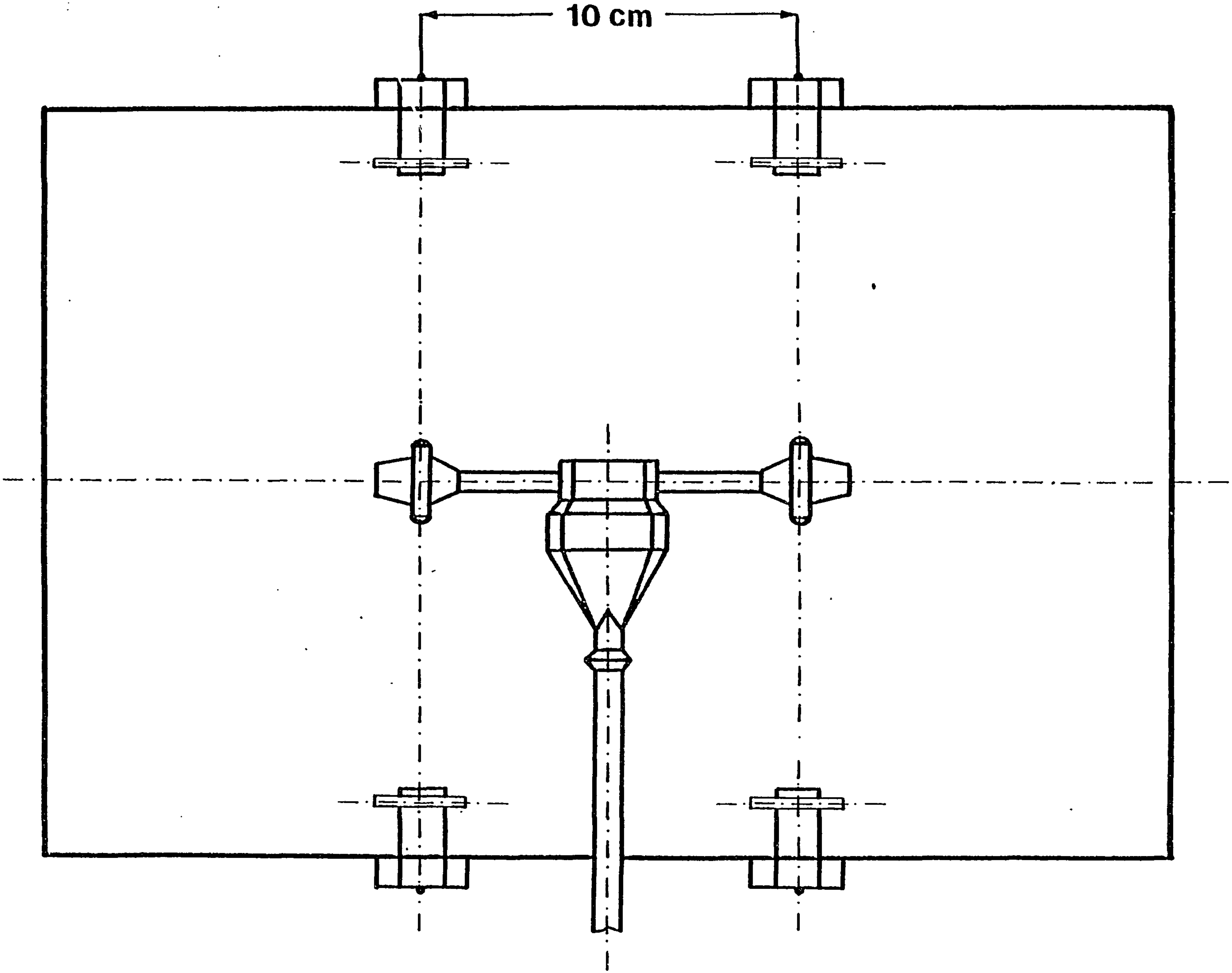

Fig. 5

Fig. 6

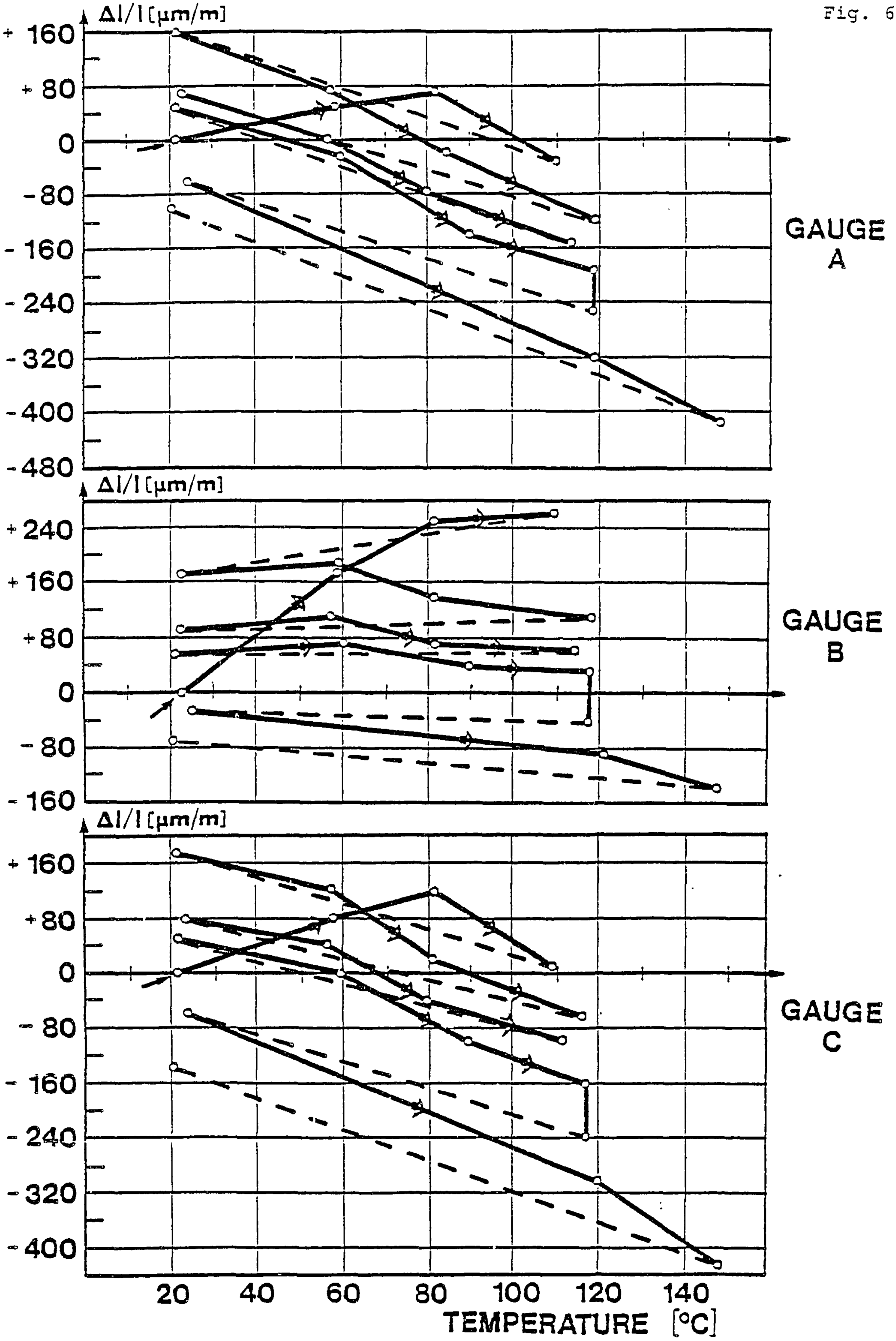

Δl/l [µm/m]
+160
+80
0
-80
-160
-240
-320
-400
-480
GAUGE A
Δl/l [µm/m]
+240
+160
+80
0
-80
-160
GAUGE B
Δl/l [µm/m]
+160
+80
0
-80
-160
-240
-320
-400
GAUGE C
20
40
60
80
100
120
140
TEMPERATURE [°C]

Fig. 7

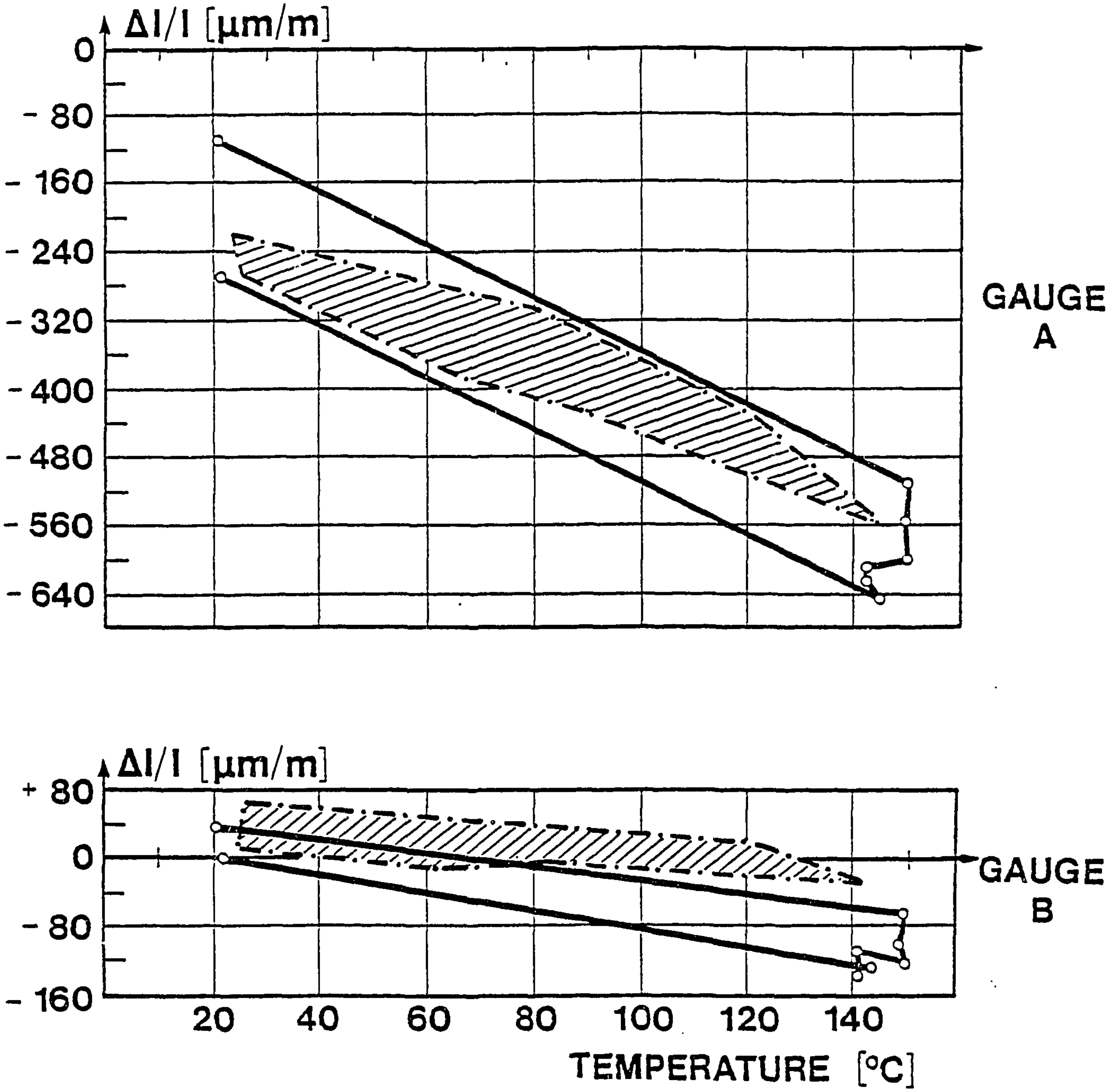

Δl/l [μm/m]
0
- 80
- 160
- 240
- 320
- 400
- 480
- 560
- 640
GAUGE A
Δl/l [μm/m]
+ 80
0
- 80
- 160
GAUGE B
20
40
60
80
100
120
140
TEMPERATURE [°C]

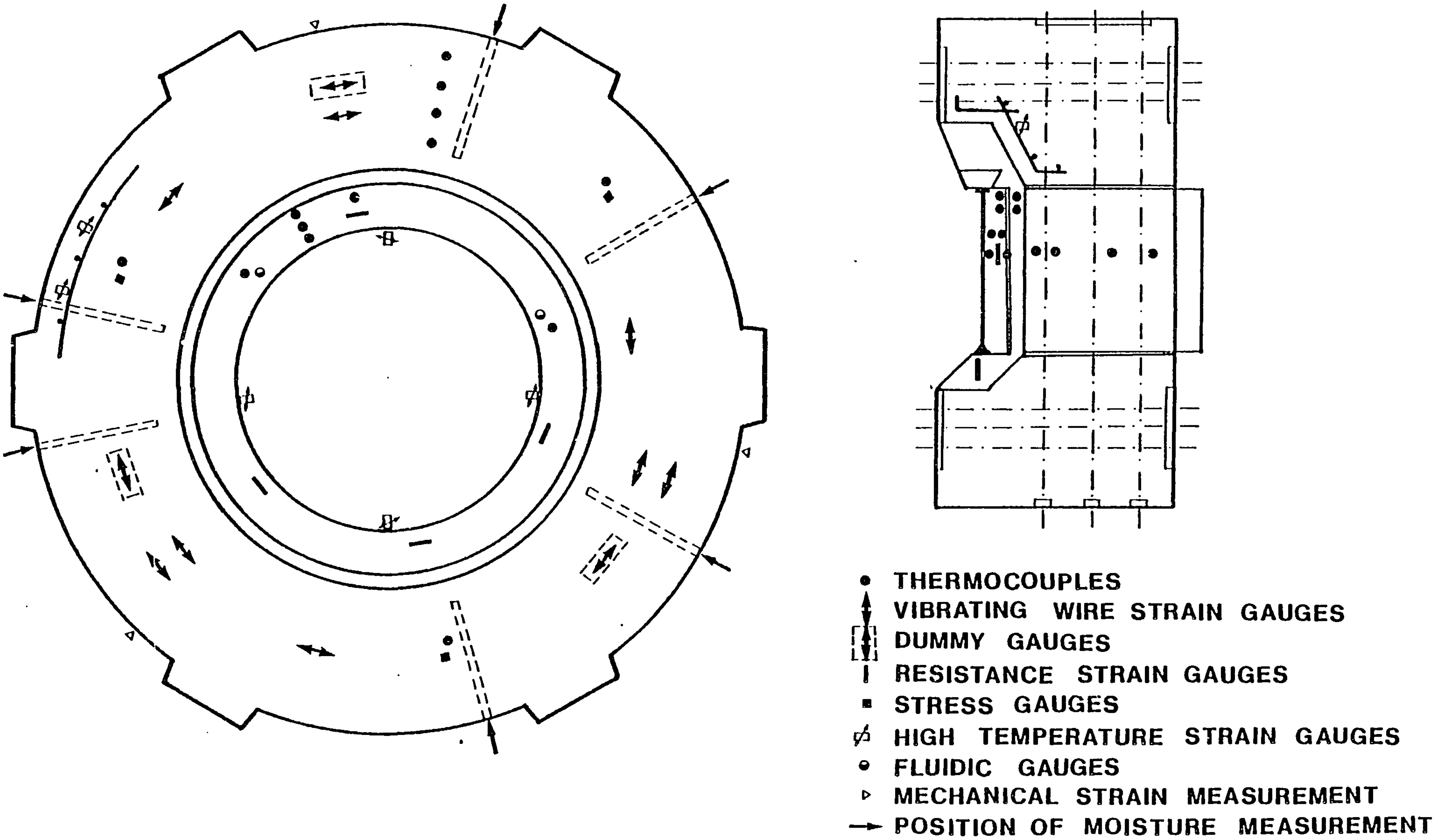
THERMOCOUPLES
VIBRATING WIRE STRAIN GAUGES
DUMMY GAUGES
RESISTANCE STRAIN GAUGES
STRESS GAUGES
HIGH TEMPERATURE STRAIN GAUGES
FLUIDIC GAUGES
MECHANICAL STRAIN MEASUREMENT
POSITION OF MOISTURE MEASUREMENT

Fig. 8

Fig. 9

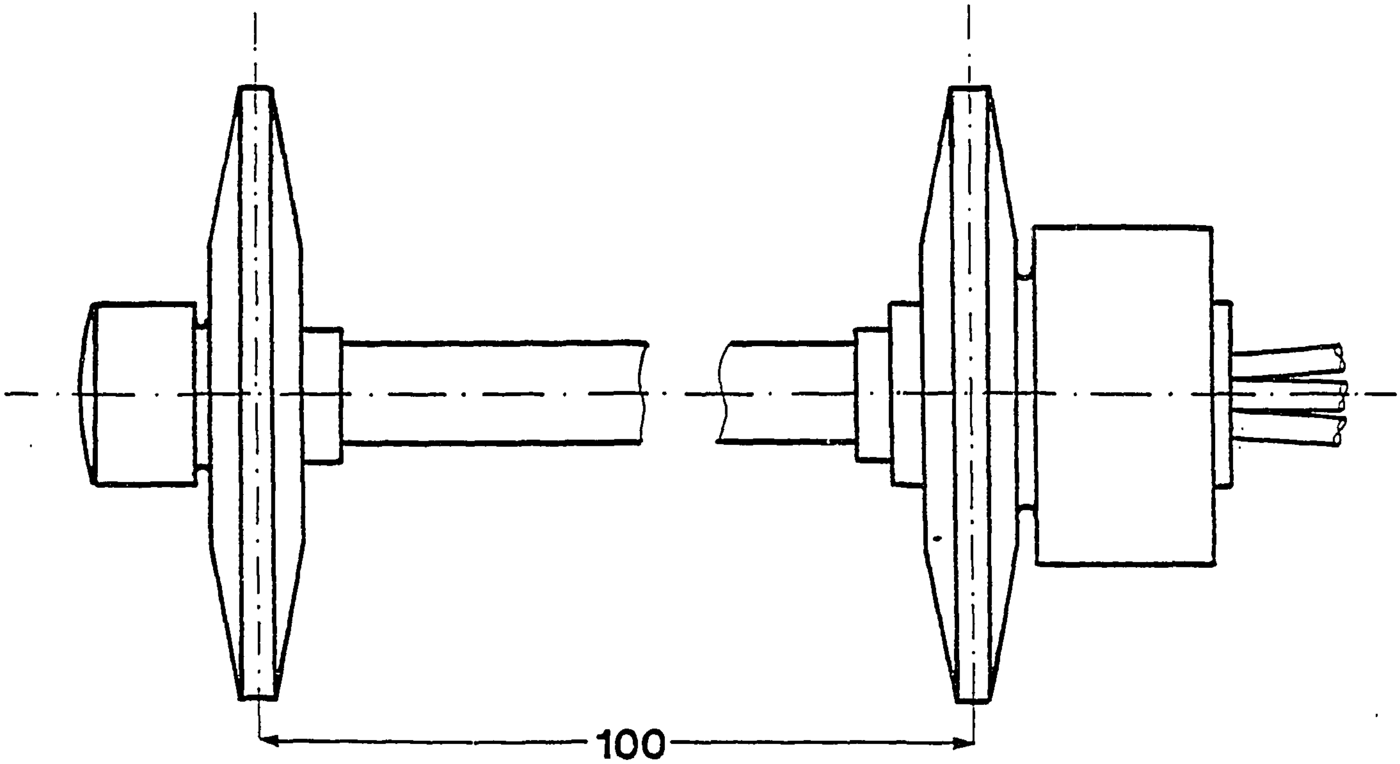

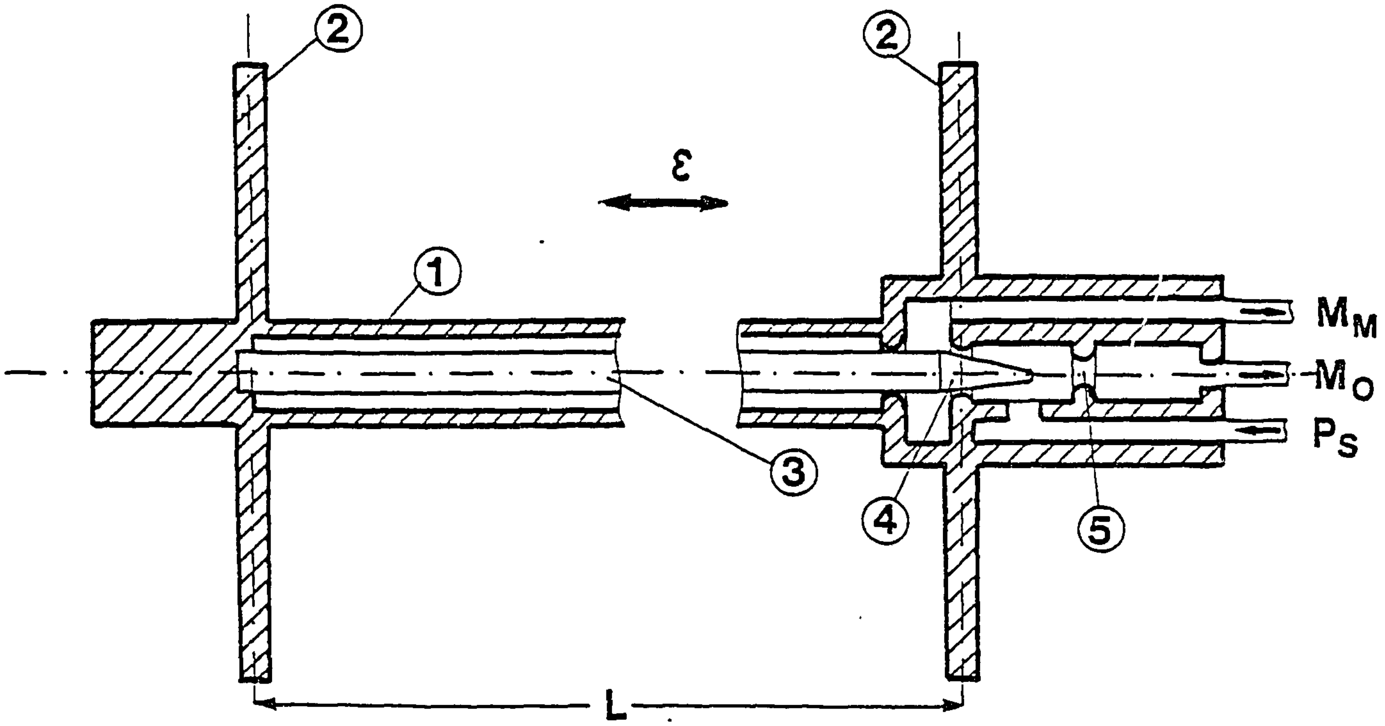

Fig. 1o

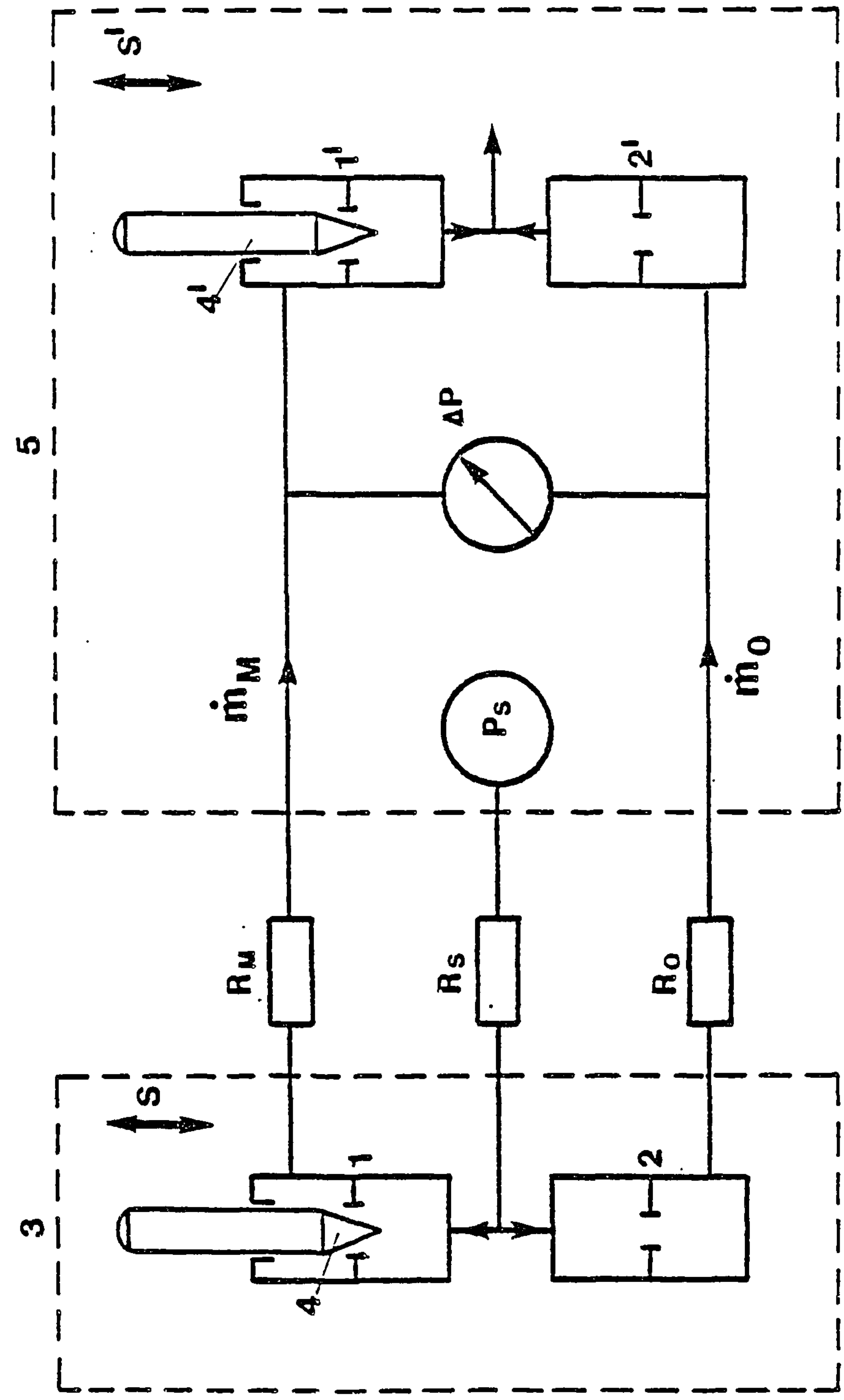

Fig. 11

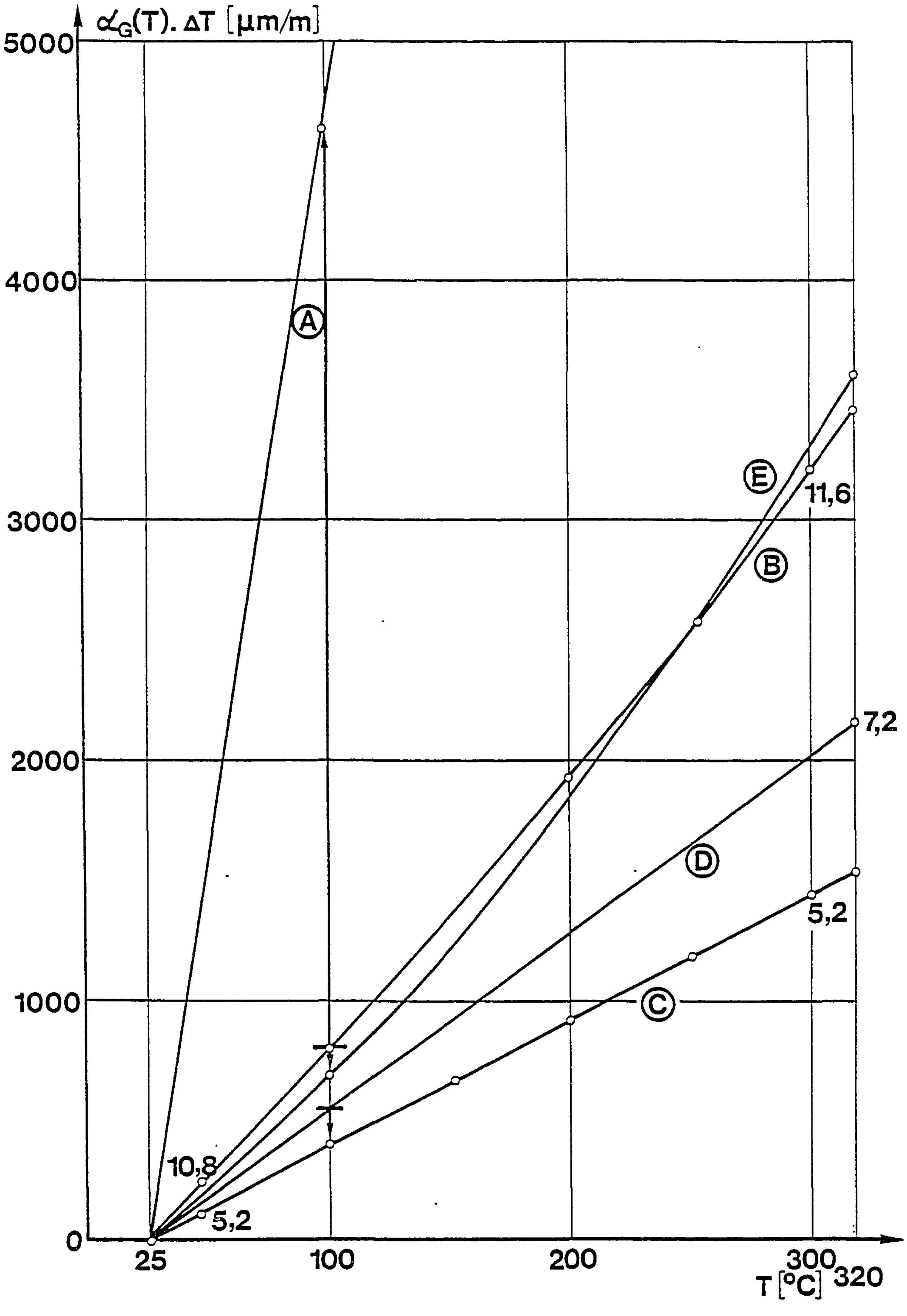

αG(T). ΔT [µm/m]
5000
4000
3000
2000
1000
0
25
100
200
300
320
T [°C]
A
B
C
D
E
11,6
7,2
5,2
10,8
5,2

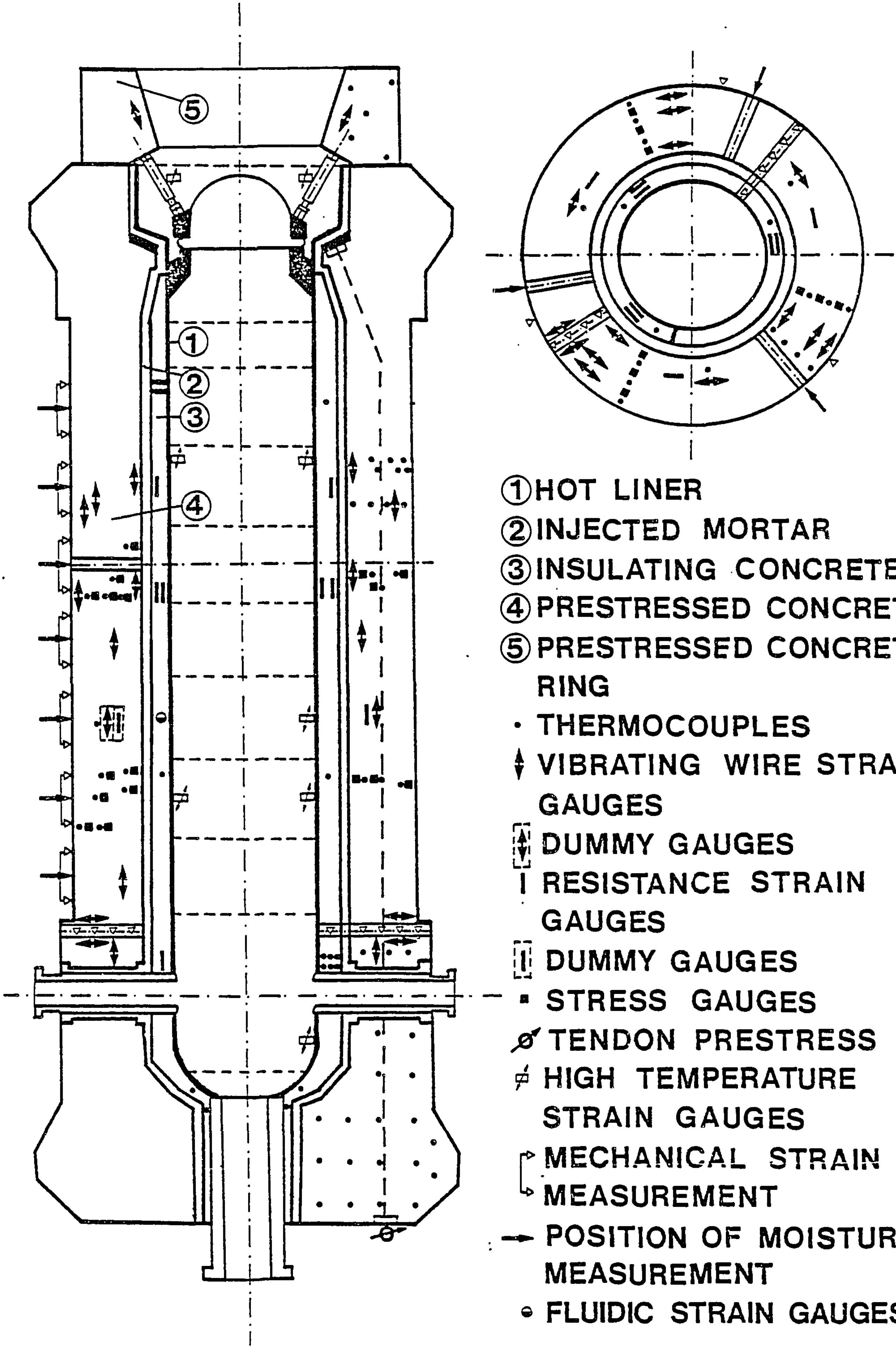

①HOT LINER
②INJECTED MORTAR
③INSULATING CONCRETE
④PRESTRESSED CONCRETE
⑤PRESTRESSED CONCRETE RING
· THERMOCOUPLES
VIBRATING WIRE STRAIN GAUGES
DUMMY GAUGES
RESISTANCE STRAIN GAUGES
DUMMY GAUGES
▪ STRESS GAUGES
TENDON PRESTRESS
HIGH TEMPERATURE STRAIN GAUGES
MECHANICAL STRAIN MEASUREMENT
POSITION OF MOISTURE MEASUREMENT
FLUIDIC STRAIN GAUGES

Fig. 13

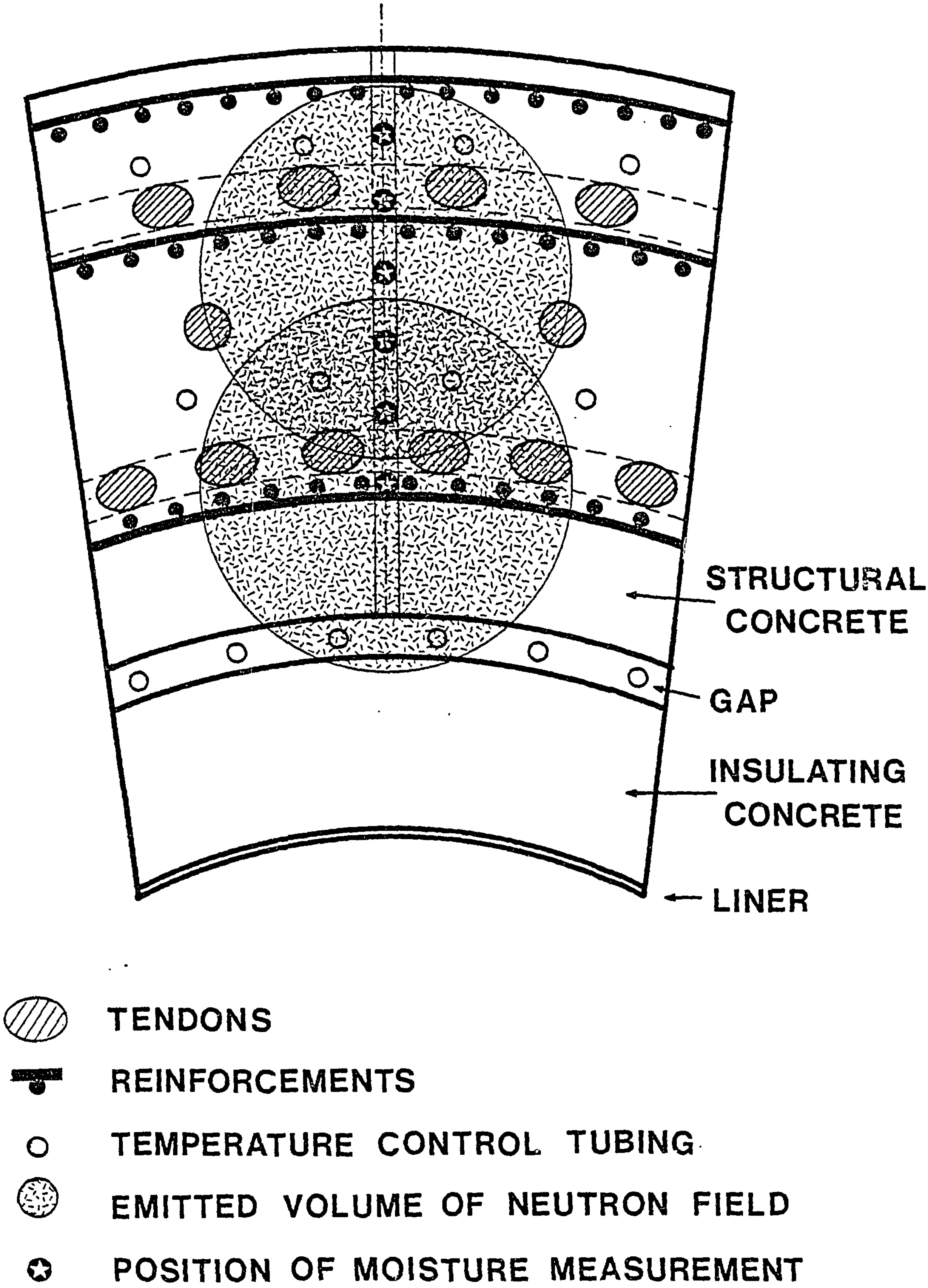

STRUCTURAL CONCRETE
GAP
INSULATING CONCRETE
LINER
TENDONS
REINFORCEMENTS
TEMPERATURE CONTROL TUBING
EMITTED VOLUME OF NEUTRON FIELD
POSITION OF MOISTURE MEASUREMENT

Fig. 14

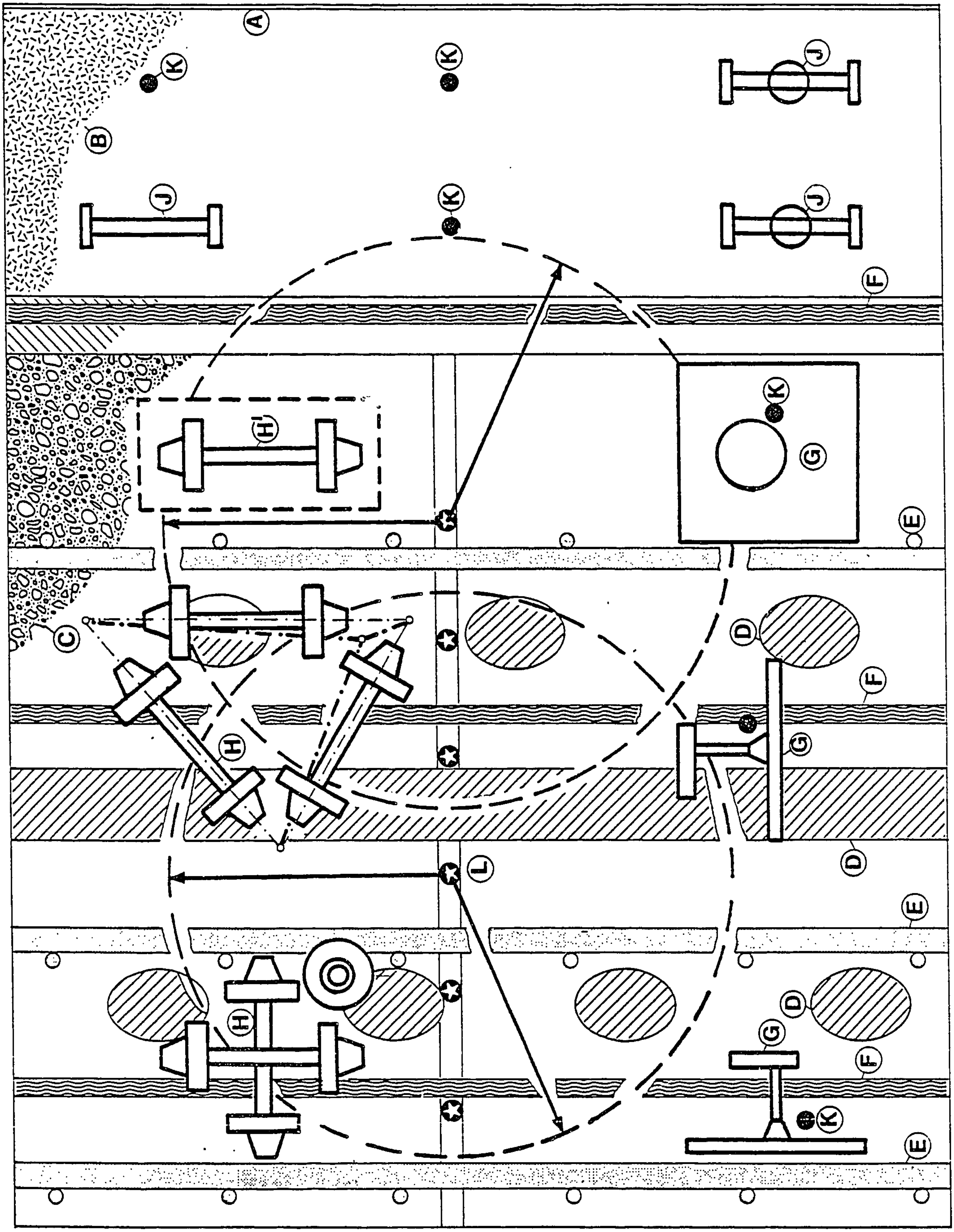

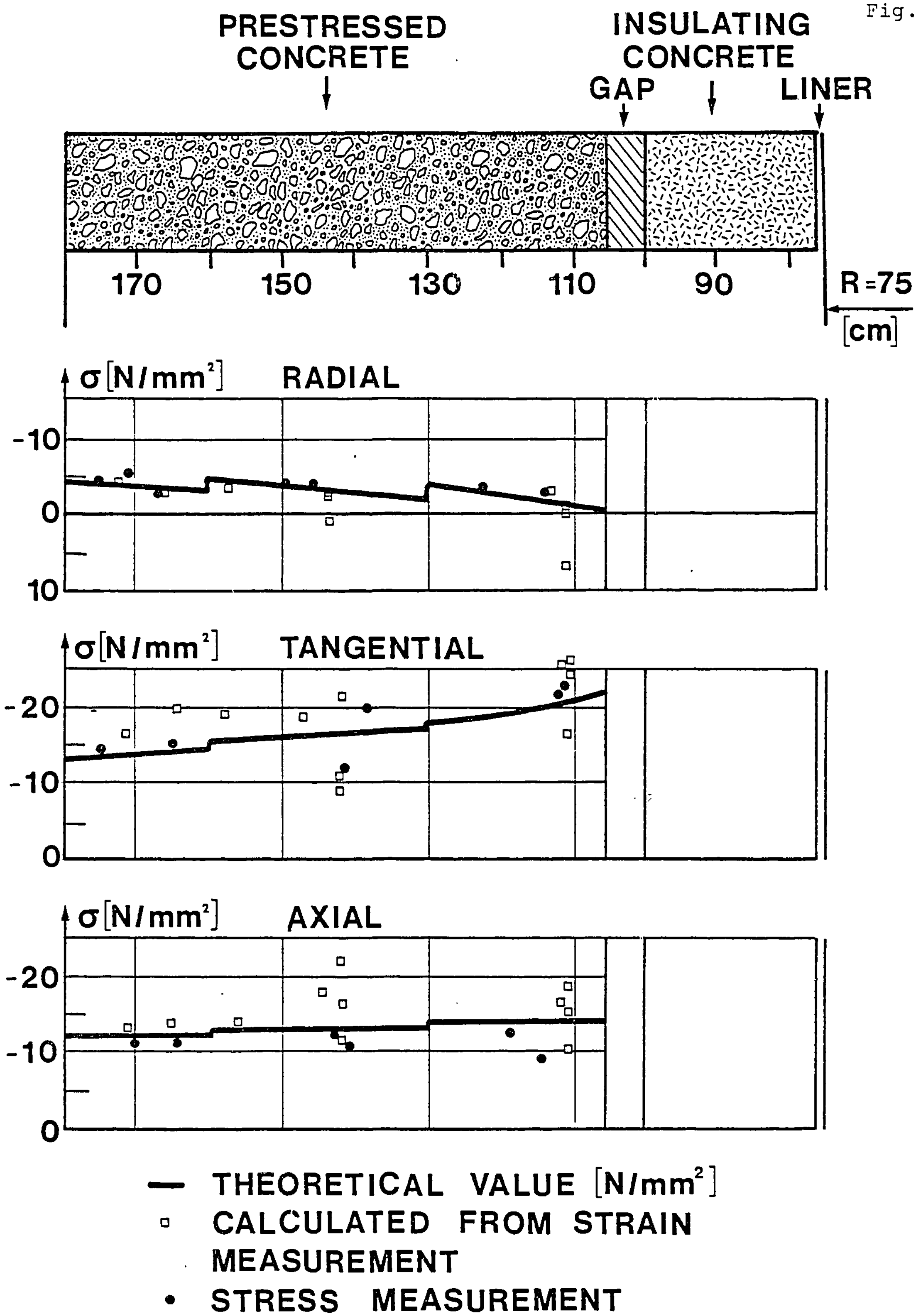
PRESTRESSED CONCRETE
INSULATING CONCRETE
GAP
LINER
170
150
130
110
90
R=75
[cm]
σ[N/mm²] RADIAL
-10
0
10
σ[N/mm²] TANGENTIAL
-20
-10
0
σ[N/mm²] AXIAL
-20
-10
0
THEORETICAL VALUE [N/mm²]
CALCULATED FROM STRAIN MEASUREMENT
STRESS MEASUREMENT

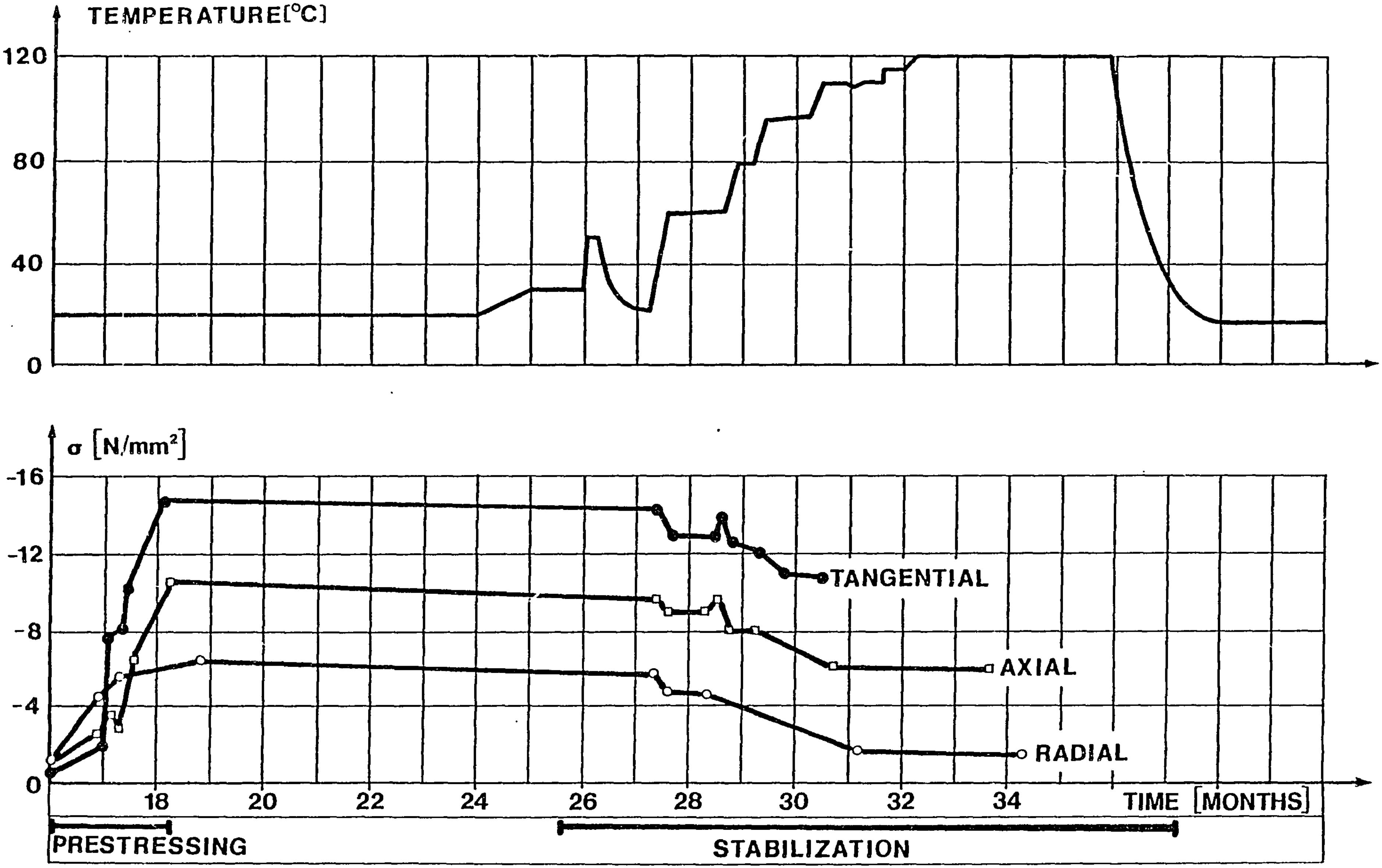
TEMPERATURE[°C]
120
80
40
0
σ [N/mm²]
-16
-12
-8
-4
0
18
20
22
24
26
28
30
32
34
TIME [MONTHS]
TANGENTIAL
AXIAL
RADIAL
PRESTRESSING
STABILIZATION

Fig. 16

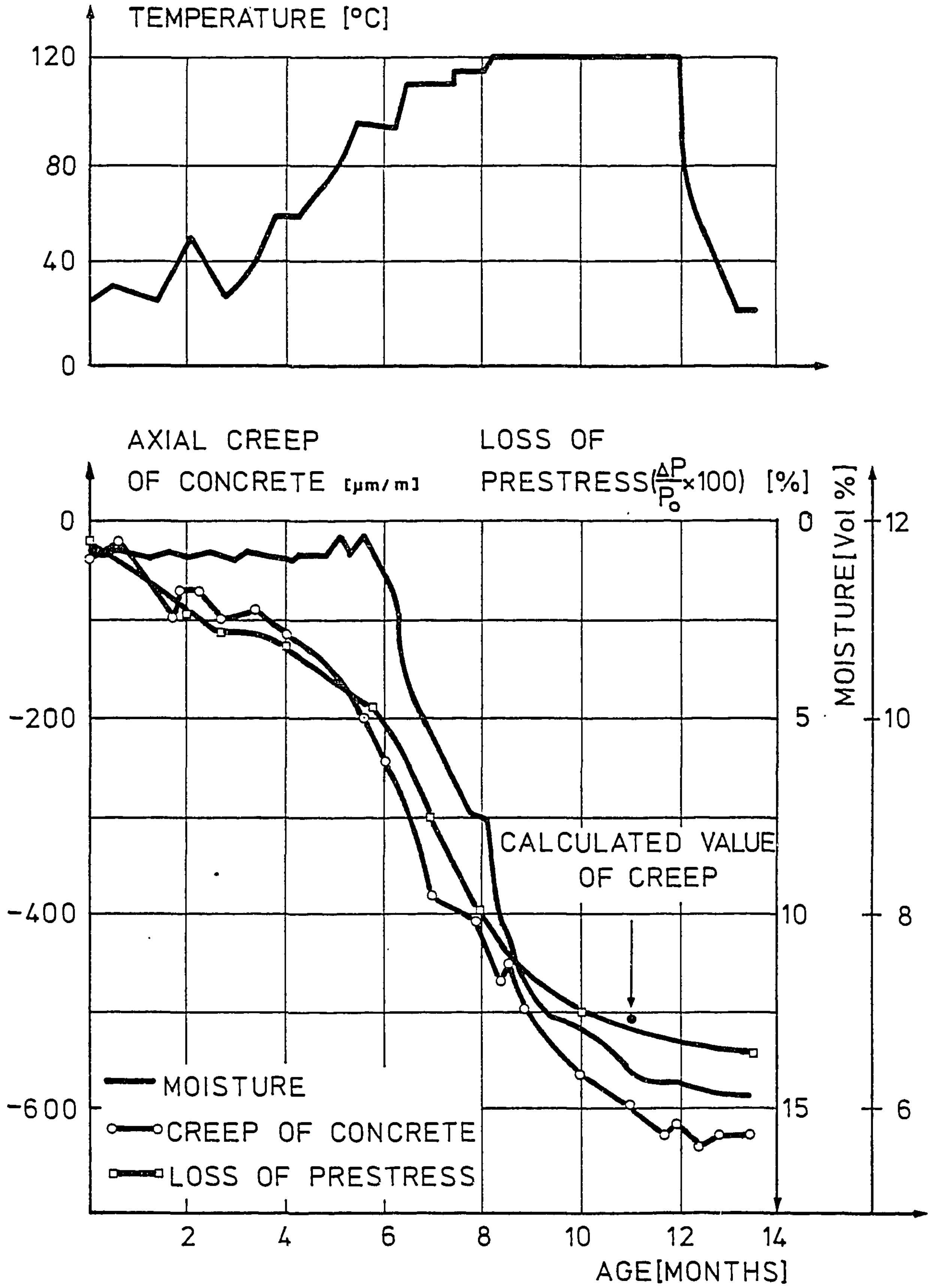
TEMPERATURE [°C]
120
80
40
0
AXIAL CREEP
OF CONCRETE [μm/m]
LOSS OF
PRESTRESS($\frac{\Delta P}{P_o}$×100) [%]
MOISTURE [Vol %]
0
-200
-400
-600
0
5
10
15
12
10
8
6
CALCULATED VALUE
OF CREEP
MOISTURE
CREEP OF CONCRETE
LOSS OF PRESTRESS
2
4
6
8
10
12
14
AGE [MONTHS]

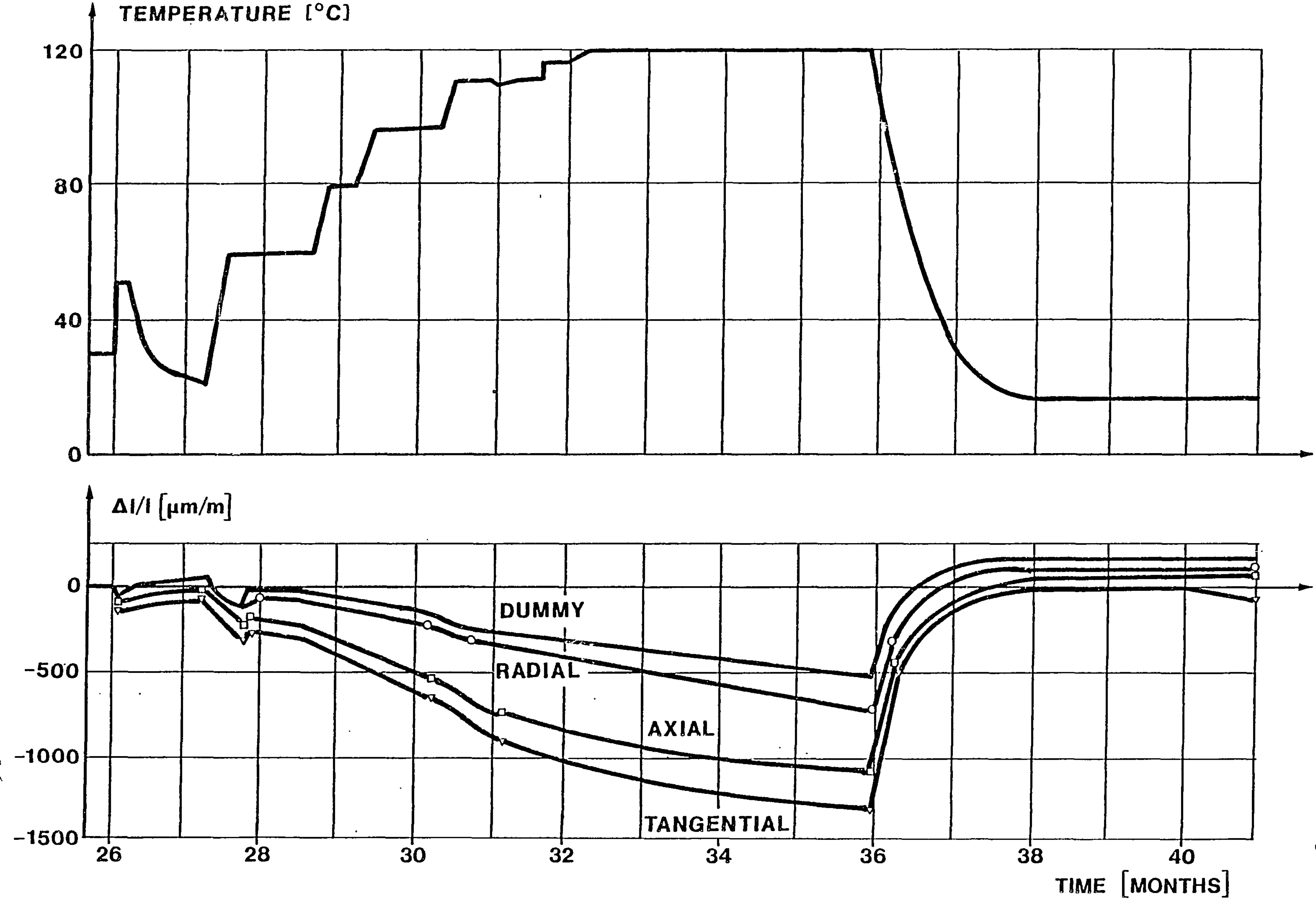
TEMPERATURE [°C]
120
80
40
0
Δl/l [μm/m]
0
-500
-1000
-1500
DUMMY
RADIAL
AXIAL
TANGENTIAL
26
28
30
32
34
36
38
40
TIME [MONTHS]

Fig. 18

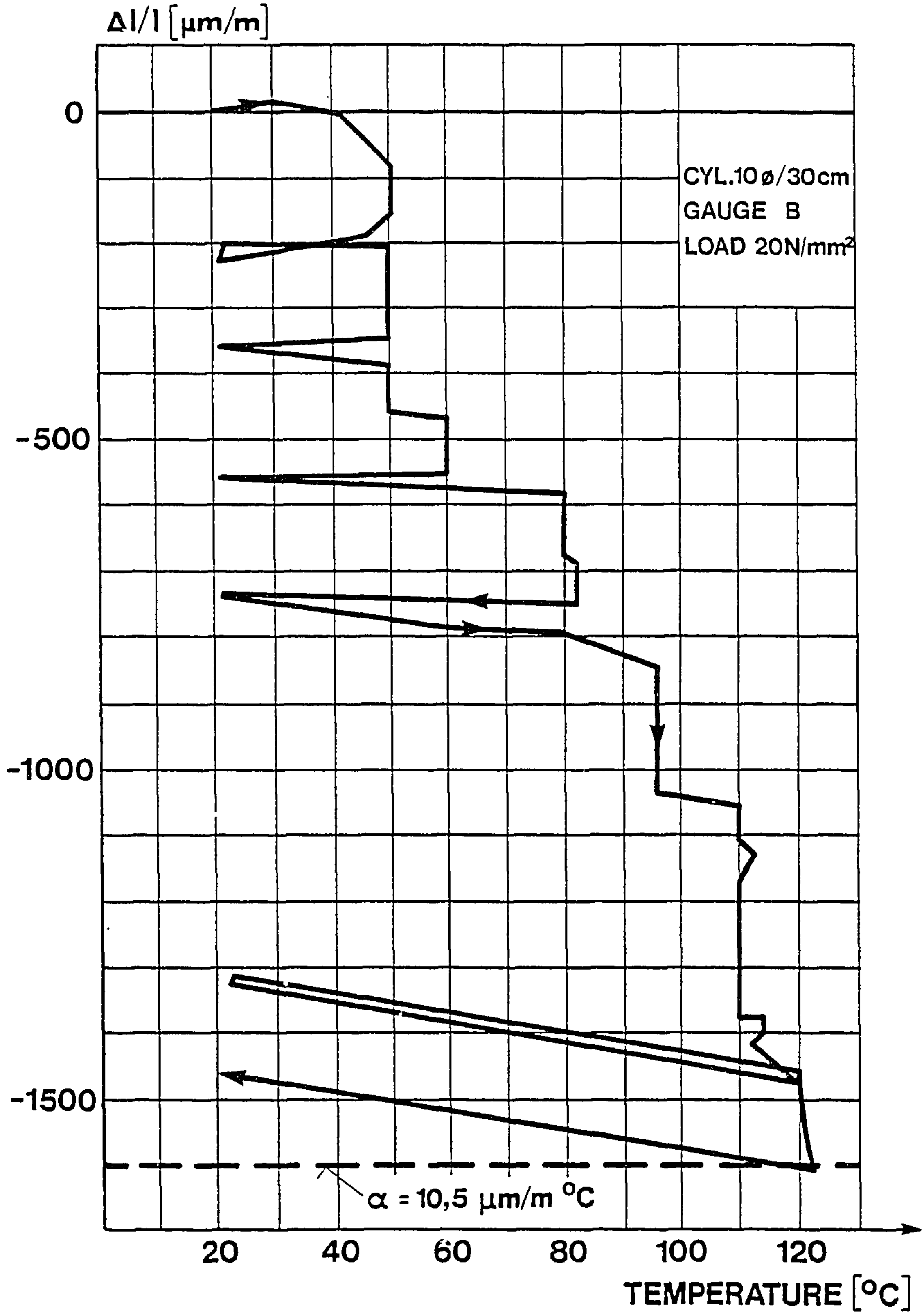
Δl/l [µm/m]
0
-500
-1000
-1500
CYL.10ø/30cm
GAUGE B
LOAD 20N/mm²
α = 10,5 µm/m °C
20
40
60
80
100
120
TEMPERATURE [°C]

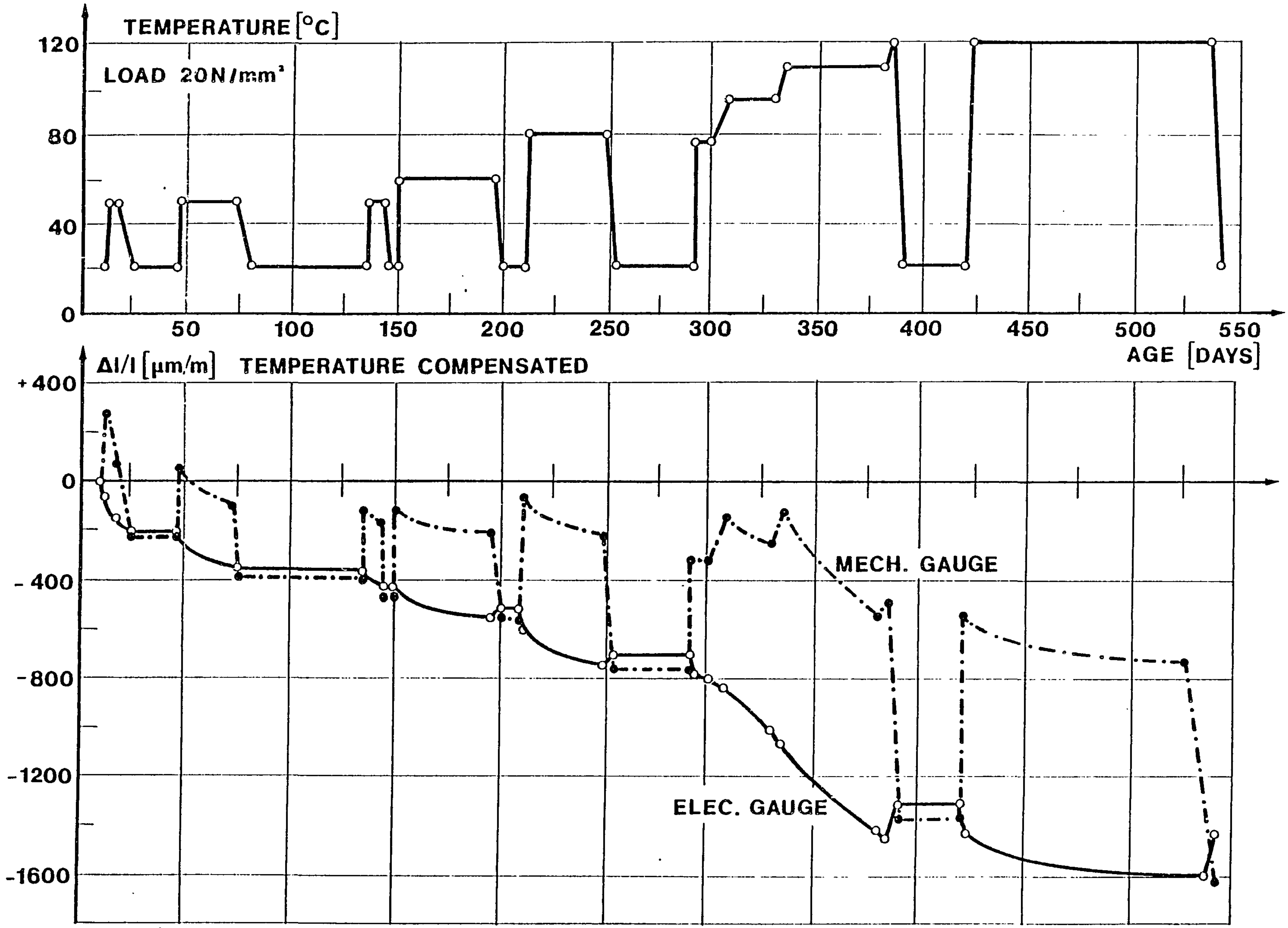
TEMPERATURE [°C]
LOAD 20N/mm²
120
80
40
0
50
100
150
200
250
300
350
400
450
500
550
AGE [DAYS]
Δl/l [μm/m] TEMPERATURE COMPENSATED
+400
0
-400
-800
-1200
-1600
MECH. GAUGE
ELEC. GAUGE

Fig. 20

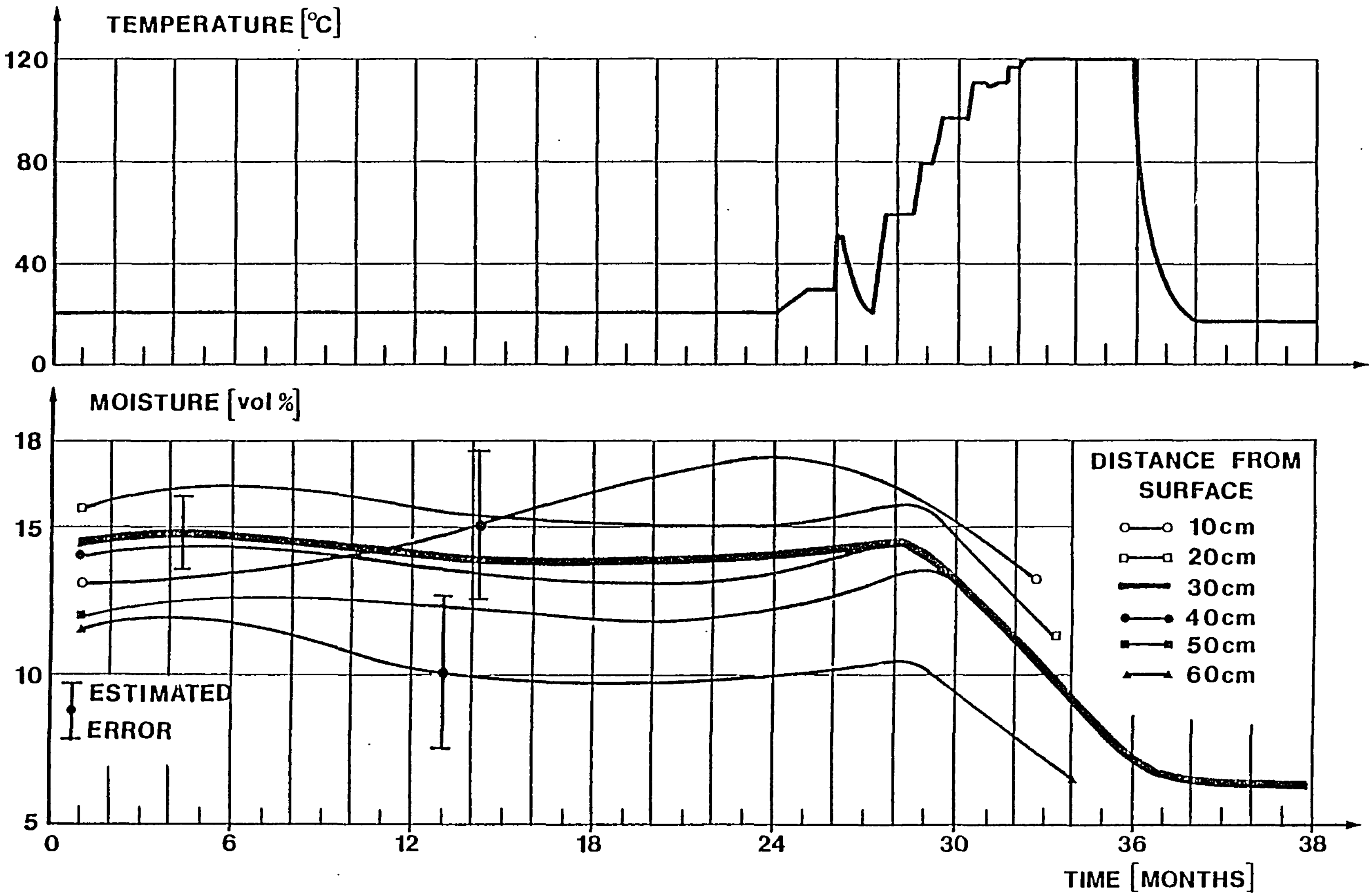
TEMPERATURE [°C]
120
80
40
0
MOISTURE [vol %]
18
15
10
5
0
6
12
18
24
30
36
38
TIME [MONTHS]
DISTANCE FROM SURFACE
10cm
20cm
30cm
40cm
50cm
60cm
ESTIMATED ERROR

Fig. 21

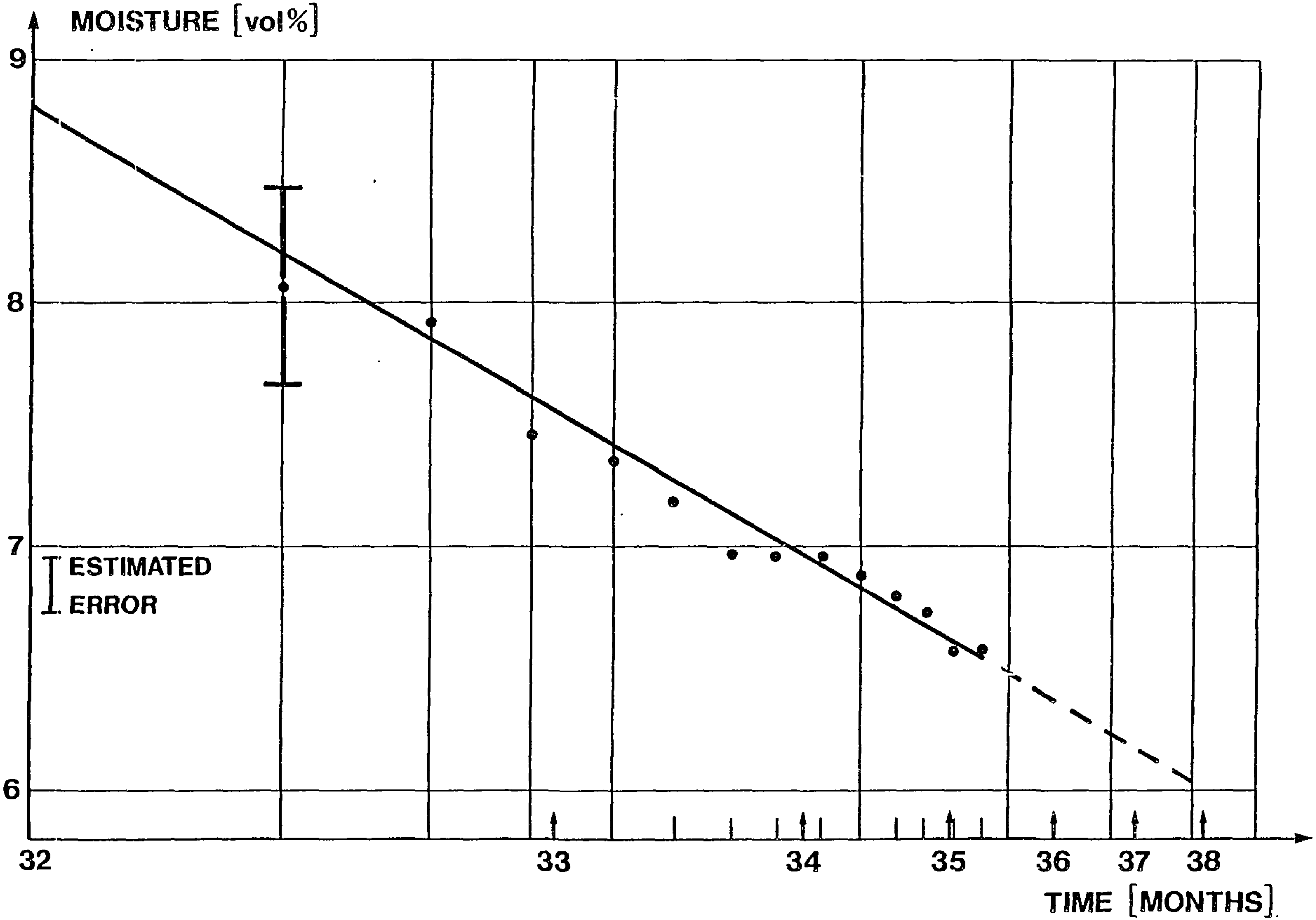

MOISTURE [vol%]
9
8
7
6
ESTIMATED ERROR
32
33
34
35
36
37
38
TIME [MONTHS]

Fig. 22

Fig. 23

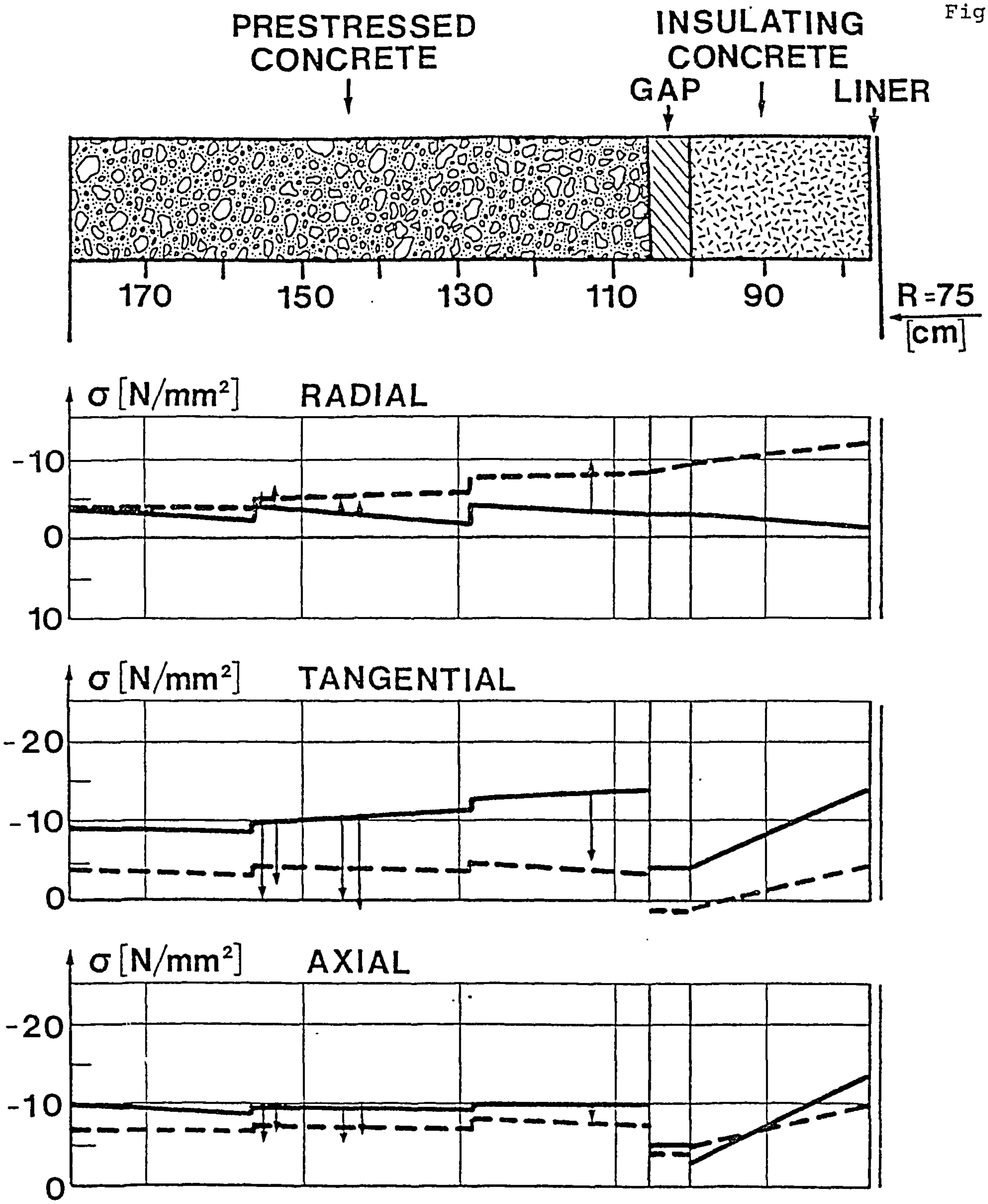

THEORETICAL VALUE [N/mm²]: —— 0 BAR } INNER
- - - 115 BAR } PRESSURE

↓ CHANGES OF STRESS CALCULATED FROM STRAIN MESUREMENTS

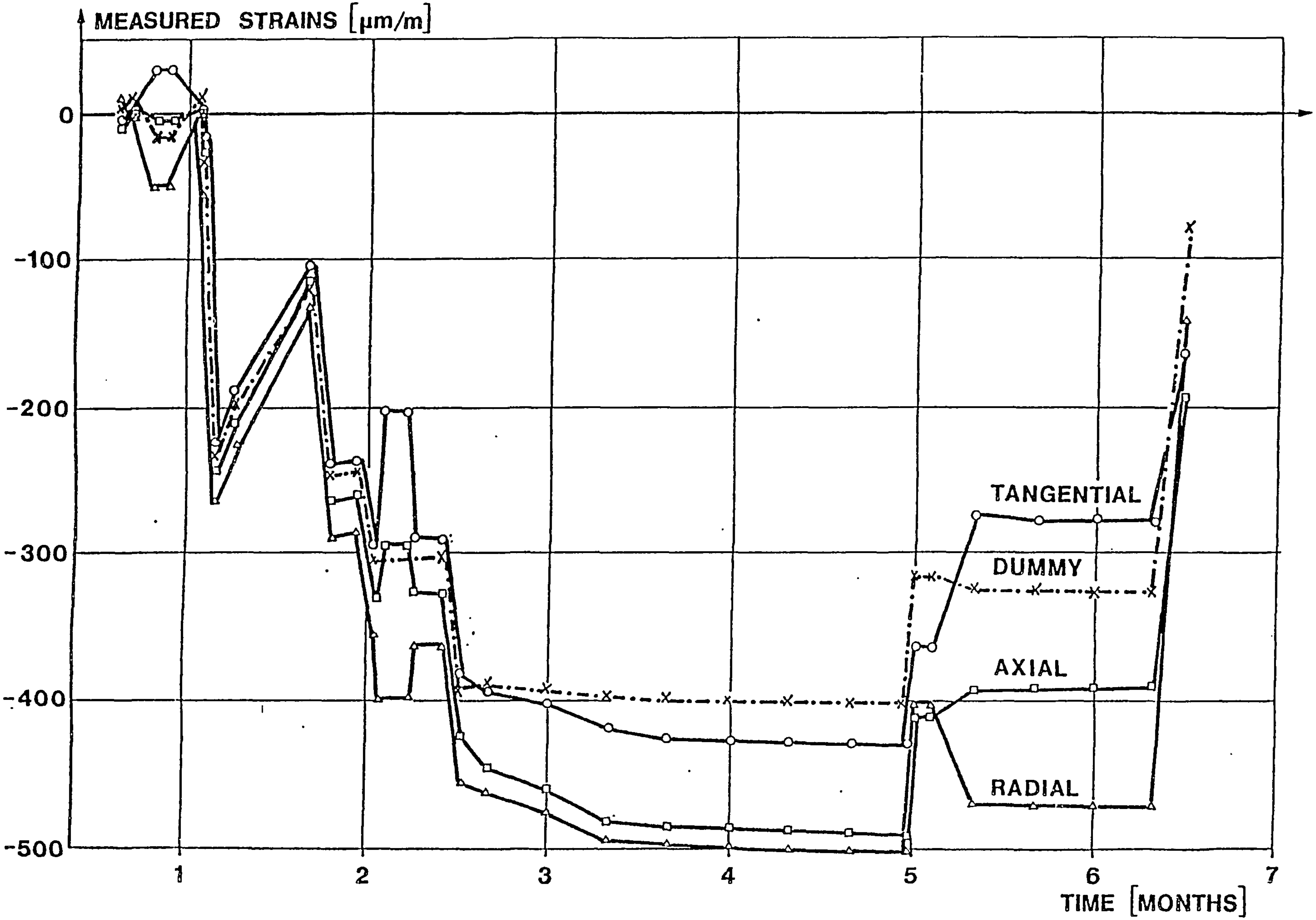
MEASURED STRAINS [μm/m]
0
-100
-200
-300
-400
-500
1
2
3
4
5
6
7
TIME [MONTHS]
TANGENTIAL
DUMMY
AXIAL
RADIAL

Fig. 24b

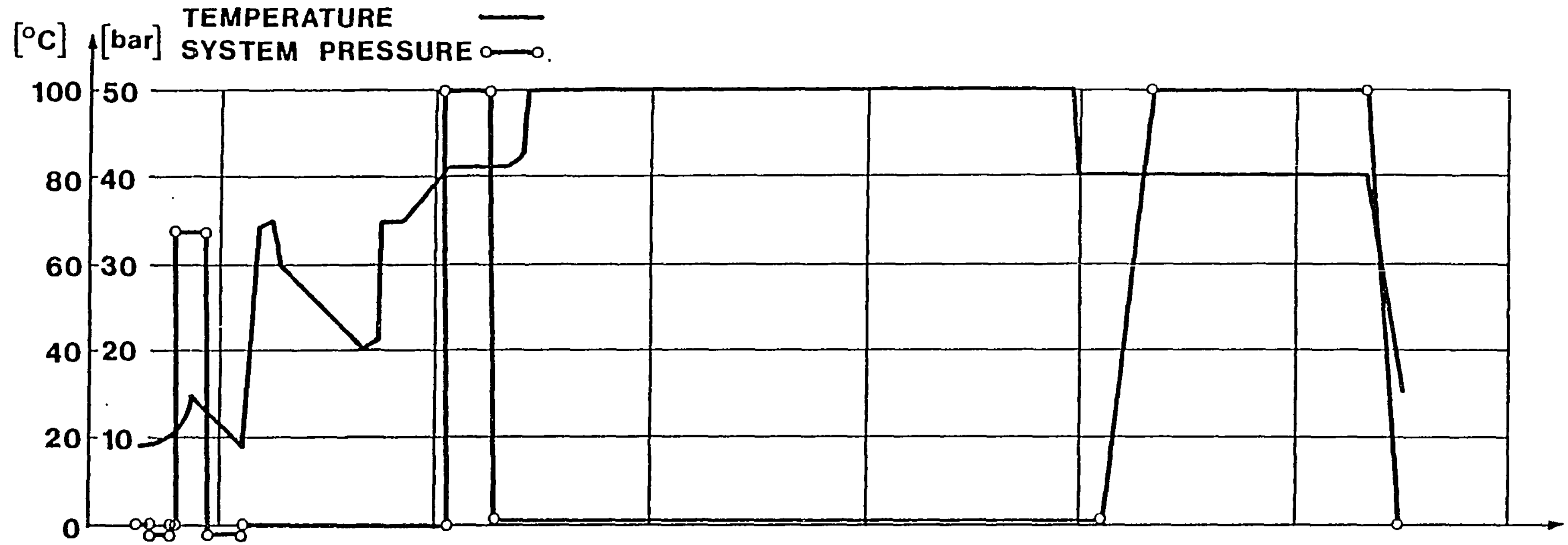

Fig. 24a

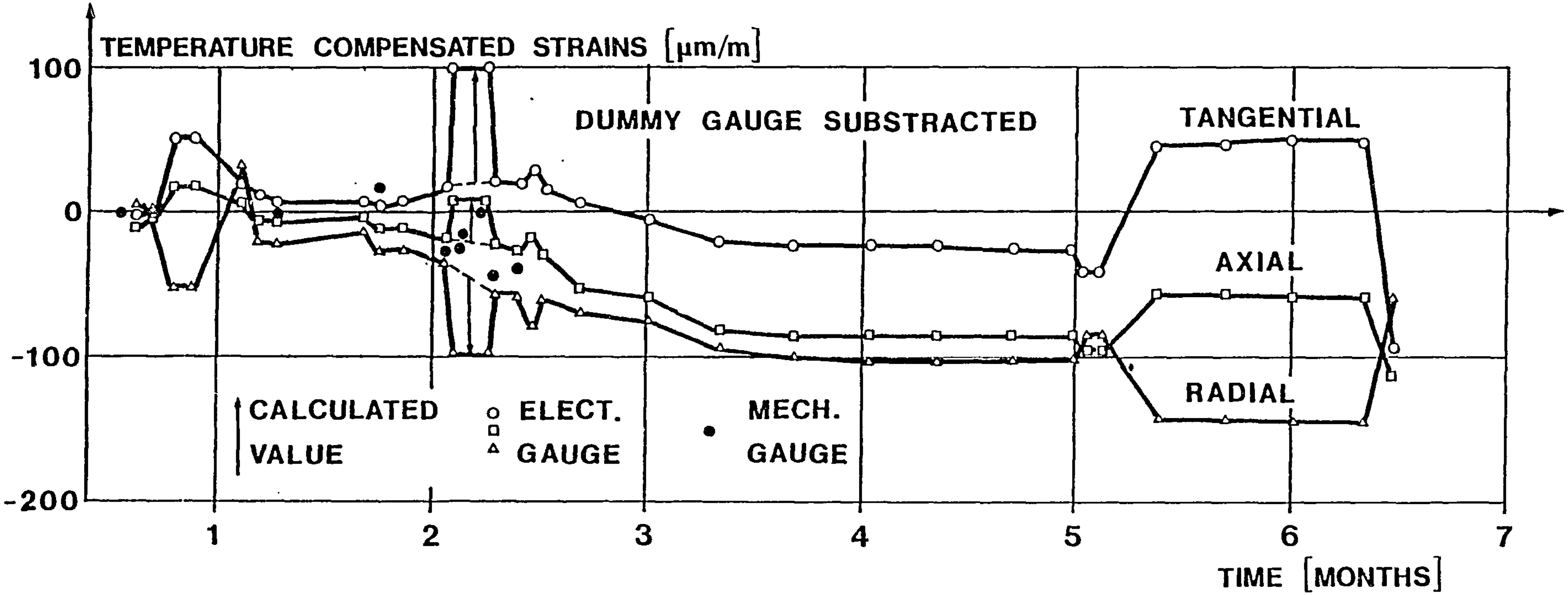

Fig. 24c

OEFZS-Berichte
Verleger, Herausgeber und Hersteller:
Österreichisches Forschungszentrum Seibersdorf Ges.m.b.H.
Redaktion: Univ. Prof. Dr. Peter KOSS,
alle Lenaugasse 10, 1082 Wien, Tel. (0222) 42 75 11, Telex 7-5400.